

ABSTRACT

JOHNSON, CHRISTOPHER MILES. Novel Material for Detection of Pathogens, Chemical Warfare Agents, and Biological Threats. (Under the direction of Drs. Saad Khan and Julie Willoughby).

Due to the frequent threat of pathogen attack, intentional or unintentional, and the potential for catastrophic effects from chemical and biological attack, quick, effective, and easy to use detection systems are a must. Current detection methods are either too slow, require additional work to be useful, or are not user friendly. In order to satisfy a growing need for improved detection systems, we have investigated the use of polyaniline, a conducting polymer with color changing ability associated with its several oxidation states, as a detector for pathogen and chemical/biological threat detection. Using interfacial polymerization to polymerize polyaniline, we developed a colorimetric sensor for use in pathogen detection. Dispersing polyaniline in a 0.25 mM hydrogen peroxide solution, we were able to demonstrate the detection of horseradish peroxidase by visually observing color change through the catalytic oxidation of polyaniline by hydrogen peroxide, and verify the results analytically via UV-VIS spectroscopy. We found the polyaniline based sensor achieved the lower detection limit of 5.5×10^{-10} M HRP at a rate of 40 minutes. The reaction conditions were an operating temperature of 23°C, PANI concentration of 1.35 mM, H₂O₂ concentration of 0.25 mM, pH of 6.4, and constant agitation.

For use as a chemical and biological threat sensor, it is desired to design a fibrous mat capable of detecting either gases or liquid. To that extent polyaniline was grafted to two substrates of differing surface dynamic properties, poly(dimethylsiloxane) and polypropylene. Polyaniline was grafted to the substrates via *in situ* chemical oxidative polymerization through the use of a silane coupling agent, 3-

(phenylaminopropyl)trimethoxysilane. The substrate surfaces were modified via ultraviolet/ozone treatment (UVO) to facilitate the silylation of the substrates with the coupling agent. Polyaniline was then grafted to the silylated substrates at aniline moiety end of the coupling agent. Sessile contact angle, Fourier Transform Infrared Spectroscopy in the Attenuated Reflection Mode (FTIR-ATR), and optical methods confirmed the presence of polyaniline on the substrates.

© Copyright 2012 by Christopher Miles Johnson

All Rights Reserved

Novel Material for Detection of Pathogens, Chemical Warfare Agents, and Biological Threats

by
Christopher Miles Johnson

A thesis submitted to the Graduate Faculty of
North Carolina State University
in partial fulfillment of the
requirements for the degree of
Master of Science

Chemical Engineering

Raleigh, North Carolina

2012

APPROVED BY:

Saad A. Khan
Co-Committee Chair

Julie Willoughby
Co-Committee Chair

Michael D. Dickey

DEDICATION

To my wonderful wife, Lynda.

Thanks for all your love and support.

BIOGRAPHY

Chris Johnson was born in Pittsburgh, PA and was raised in Cape Coral, FL. After graduating from Fort Myers High School, he attended the United States Military Academy at West Point, NY. After graduating with a Bachelor of Science degree in Chemistry in 2001, he was commissioned a Second Lieutenant in the Air Defense Artillery branch of the United States Army. After three years in the Air Defense Artillery branch, Chris became a Military Intelligence Officer. He has been stationed in Germany, Arizona, and Texas, serving in several different duty positions, including Platoon Leader, Battery Executive Officer, and Company Commander. Starting in the Fall of 2010, Chris began attending North Carolina State University to obtain a Master of Science degree from the Department of Chemical and Biological Engineering. He joined the research group led by Dr Saad Khan in 2011 and was co-advised by Dr Juilie Willoughby from the College of Textiles. Following completion of his studies, Chris will join the Department of Chemistry at the United States Military Academy as West Point.

ACKNOWLEDGMENTS

First and foremost I would like to thank my advisors, Dr Khan and Dr Willoughby. Thank you for your advice, ideas, and guidance. Without you, this would have been a much more difficult process.

Thank you to all the members of the Khan Research Group and the Willoughby Research Group. Thanks especially to the undergrads and high school students that worked alongside me on my projects. Thank you also to Dr Sara Arvidson, Christina Tang, and Alina Higham for their help and assistance on conducting research and providing constructive comments for products resulting from the research.

Thank you to the U.S. Army for giving me the opportunity to attend graduate school and obtain an advanced degree.

Last, but certainly not least, I would like to thank my wife for her continued love, support, and understanding throughout our young marriage.

TABLE OF CONTENTS

LIST OF TABLES	vii
LIST OF FIGURES	viii
CHAPTER 1: Introduction	1
1.1 Motivation	1
1.1.1 Pathogen detection	1
1.1.2 Chemical warfare agent detection	2
1.1.3 Polyaniline	3
1.2 Research goals and thesis organization	6
REFERENCES	10
CHAPTER 2: Dispersion Based Sensor	13
2.1 Introduction	13
2.1.1 Detection system overview	14
2.1.2 Horseradish peroxidase and hydrogen peroxide	15
2.1.3 Polyaniline	16
2.2 Materials and Methods	16
2.2.1 Materials	16
2.2.2 Polyaniline polymerization	17
2.2.3 Purification of PANI	17
2.2.4 Scanning Electron Microscopy (SEM)	18
2.2.5 Ultraviolet-Visible Spectroscopy (UV-VIS)	18
2.3 Results and Discussion	18
2.3.1 Polyaniline polymerization	18
2.3.2 Determining optimum H ₂ O ₂ concentration	20
2.3.3 Determining optimum pH	22
2.3.4 Effect of temperature on HRP detection	23
2.3.5 Effect of constant agitation	25
2.4 Conclusions and Future Work	26
REFERENCES	42
CHAPTER 3: Solid Based Detection System	45
3.1 Introduction	45
3.1.1 Polydimethylsiloxane and polypropylene	45
3.1.2 Previous work on grafting PANI	46
3.2 Materials and Methods	47
3.2.1 Materials	47
3.2.2 Ultraviolet Ozone (UVO) Treatment	48
3.2.3 Silylation	48
3.2.4 Polyaniline graft polymerization	48
3.2.5 Contact angle measurements	49

3.2.6 Fourier Transform Infrared Spectroscopy in the Attenuated Reflection Mode.....	50
3.3 Results and Discussion.....	50
3.3.1 UVO treatment of PDMS and PP	50
3.3.2 Silylation of PP and PDMS	51
3.3.3 Polyaniline graft polymerization.....	53
3.3.4 Exposure to ammonia hydroxide vapor	56
3.4 Conclusions and future work.....	56
REFERENCES	70
CHAPTER 4: Conclusions and Future Work.....	72
4.1 Conclusions.....	72
4.1.1 Pathogen detection system.....	72
4.1.2 Chemical warfare agent detection.....	74
4.2 Future work.....	75
4.2.1 Pathogen detection system.....	75
4.2.2 Chemical warfare agent detection.....	76
REFERENCES	78

LIST OF TABLES

Table 3.1 Average contact angles of PDMS and PP before UVO, after UVO, and after silylation with PAPTMOs, with standard deviation (SD).....	60
--	-----------

LIST OF FIGURES

Figure 1.1 Common military chemical warfare agent detectors. (a) M22 Chemical Agent Alarm; (b) Improved Chemical Agent Monitor; (c) M9 paper 8

Figure 1.2 Various oxidation states of PANI, colors associated with the oxidation states, and the chemical routes that lead to each oxidation state. 9

Figure 2.1 Overview of pathogen detection system. (a) Capture antibodies are immobilized on a fiber mat. (b) The mat is exposed to a sample. (c) If a pathogen is present, the capture antibodies will capture it. (d) The mat is then exposed to detection antibodies (antibodies conjugated with HRP). (e) If a pathogen is present, the detection antibodies will bind to the pathogen. (f) The mat is then placed in a PANI and H_2O_2 solution. If a pathogen is present, the HRP that is conjugated on the capture antibody that is bound to the pathogen will catalyze the oxidation of the PANI solution by H_2O_2 , causing a change in oxidation states and color of the PANI. 28

Figure 2.2 Interfacial polymerization of PANI. (a) Aniline is dissolved in the organic phase and the oxidant, ammonium persulfate, is in HCl. The aqueous oxidant solution is slowly added to the organic phase. Immediately PANI forms at the interface between the aqueous and organic phases. (b) At the completion of the reaction, PANI is dispersed in the aqueous phase and no aniline monomer remains in the organic phase. 29

Figure 2.3 Progress of interfacial polymerization of polyaniline. (a) Aniline-hydrochloride in dichloromethane before addition of aqueous phase. (b) Addition of aqueous phase. Immediately upon contact of the aqueous phase with the organic phase, red was observed. As more aqueous phase was added, the color changed from red to blue to green. (c) Completion of addition of aqueous phase. After the aqueous phase was added, the aqueous phase was green. (d) Completion of polymerization. The organic phase was dark amber, indicating completion of the reaction. The aqueous phase was dark green. 30

Figure 2.4 Polymerization of PANI. (a) Aniline cation radical formed when aniline monomer reacts with an oxidant to initiate the polymerization of PANI. (b) Resonance structures formed from the aniline cation radical. Form (ii) is most likely the most reactive species due to the availability of the radical. (c) The formation of a polyaniline dimer. The aniline cation radical reacts with one of the resonance structures of the cation radical, forming a dimer. (d) After the release of 2 hydrogens and rearrangement, the dimer becomes para-aminodiphenylamine (PADPA). PADPA is oxidized twice forming a radical dimer which then reacts with other radicals in solution, forming PANI. 31

Figure 2.5 UV-VIS spectrum of PANI in DI water after interfacial polymerization. The minimum absorbance value of 493.5 nm indicated the PANI was green in color. 32

Figure 2.6 SEM micrographs of PANI. (a) 2500x magnification, (b) 5000x magnification, (c) 10000x magnification, (d) 20000x magnification, (e) 40000x magnification, (f) 80000x magnification.	33
Figure 2.7 Effect of H ₂ O ₂ concentration on PANI. After over 25 hours, H ₂ O ₂ concentrations ≤ 0.25mM had little to no effect on the oxidation of PANI, however PANI was being oxidized after a few hours at an H ₂ O ₂ concentration of 0.50 mM.	34
Figure 2.8 The effect of different H ₂ O ₂ concentrations and different HRP concentrations on the oxidation of PANI. At an HRP concentration of 550 nM, PANI was oxidized regardless of the H ₂ O ₂ concentration (black squares and blue triangles). At an HRP concentration of 5.5 nM, 0.1 mM H ₂ O ₂ (red circle) did not oxidize PANI, however 0.25 mM H ₂ O ₂ (inverted purple triangle) did oxidize PANI.	35
Figure 2.9 Effect of pH on PANI as a function of time. H ₂ O ₂ was added after six hours....	36
Figure 2.10 Effect of increasing temperature on rate of color change for PANI at pH 6.4, 5.5 nM HRP, 0.25 mM H ₂ O ₂ . At T=4°C, color change occurred at 1683 min. At T=22°C, color change occurred at 188 min. At T=45°C, color change occurred at 30 min.	37
Figure 2.11 Arrhenius plot of oxidation of PANI at pH 6.4, 0.25 mM H ₂ O ₂ , 5.5 nM HRP, and T=4°C, 22°C, and 45°C. Using the slope of the linearly fitted line, the activation energy (E _a) was 71.9 kJ/mol.	38
Figure 2.12 Effect of temperature on PANI and 0.25 mM H ₂ O ₂ solution, without addition of HRP.	39
Figure 2.13 Images of PANI settling over time: (a) time=0; (b) time≈3 hours; (c) time≈18 hours (overnight).	40
Figure 2.14 Effect of constant agitation on the time required for color change of PANI. While under constant agitation, the PANI solutions changed color twice as fast.	41
Figure 3.1 Chemical structures for the components of chemical sensors where a) polydimethylsiloxane (PDMS) and b) polypropylene (PP) are the substrates and c) 3-(phenylaminopropyl)trimethoxysilane (PAPTMOs) is the silane coupling agent for subsequent surface grafting and polyaniline polymerization.	58
Figure 3.2 Graphical depiction of procedure to graft PANI to a substrate (PP or PDMS) using PAPTMOs. The substrate is treated with UVO for 45 minutes, generating hydrophilic groups (e.g. hydroxyls) on the surface. The modified substrate is silylated with PAPTMOs, and finally PANI is polymerized from the coupling agent.	59

Figure 3.3 Images from the OCA20 obtained during measurement of static contact angle of PDMS (a-c) and PP (d-f) before UVO treatment, after UVO treatment, and after silylation. The actual contact angle is also shown.	61
Figure 3.4 FTIR-ATR spectra of PP before and after UVO treatment. Peaks of note on the PP-OH spectrum are the peak located at 1708 cm^{-1} (C=O and -COOH) and the broad peak ranging from 3115 to 3600 cm^{-1} (-OH).....	62
Figure 3.5 FTIR-ATR spectra of PDMS before and after UVO treatment. Peaks of interest on the PDMS-OH spectrum are the peak located at 1712 cm^{-1} (C=O and -COOH) and the broad peak located from 3100 to 3600 cm^{-1} (-OH).....	63
Figure 3.6 FTIR-ATR spectra of unmodified PP and PP after silylation. Peaks of interest on the PP-PAPTAMOS spectrum are the peaks located at 1506 cm^{-1} and 1598 cm^{-1} (aromatic ring) and the broad peak centered on 3400 cm^{-1} (amine).	64
Figure 3.7 FTIR-ATR spectra of unmodified PDMS and PDMS after silylation. Peaks of interest on the PDMS-PAPTAMOS spectrum are the peaks located at 1504 cm^{-1} and 1601 cm^{-1} (aromatic ring) and the peak at 3409 cm^{-1} (amine).	65
Figure 3.8 Images of the PANI polymerization reaction vial. Image (a) is the monomer solution with a substrate in it; (b) after addition of 1 mL oxidant solution; (c) after addition of more oxidant solution; (d) after addition of 10 mL oxidant solution; (e) approximately 3 minutes after beginning to add oxidant solution.	66
Figure 3.9 Images of PDMS (a-c) and PP (d-h) throughout the PANI grafting process. a) unmodified PDMS; b) PDMS after PANI polymerization; c) PDMS after conversion to EB form and after 2 seconds in NMP; d) unmodified PP; e) PP after PANI polymerization; f) PP after conversion to EB form; g) PP after sonication in NMP; h) PP after conversion to ES form; i) PP after exposure to NH_4OH vapor.	67
Figure 3.10 FTIR-ATR spectra of PP after silylation (PP-PAPTAMOS) and after PANI polymerization (PP-PANI). The difference in the two spectra is the new peak at 1660 cm^{-1} (aromatic, amines, and imines).	68
Figure 3.11 FTIR-ATR spectra of PDMS after silylation (PDMS-PAPTAMOS) and after PANI polymerization (PDMS-PANI). There is no change to the peaks located at 1504 cm^{-1} and 1601 cm^{-1} , indicating the coupling agent is still present on the PDMS surface.....	69

CHAPTER 1: Introduction

Pathogens and chemical warfare agents continue to be a threat to people everywhere. In the US alone, pathogens affect nearly 1 in 6 lives.¹ In a similar vein, chemical weapons continue to be a constant threat all over the world, from the use of mustard gas² to the use of common gases such as chlorine³ to the use of more sophisticated weapons such as Sarin.⁴ Based on the threat, the interests of all involved are best served by the availability of threat detection systems that are easy to use, have quick response times, and are inexpensive to produce. With this end in mind, we investigate using polyaniline (PANI) as a colorimetric sensor in two potential applications, as a liquid dispersion to detect the presence of pathogens and as graft to substrates for use as a vapor sensor.

1.1 Motivation

1.1.1 Pathogen detection

According to the Center for Disease Control (CDC), the largest threat from pathogens comes from foodborne pathogens, contributing to roughly 48 million illnesses every year, resulting in approximately 3,000 deaths.¹ To prevent the spread of pathogens, quick detection methods are required. Established pathogen detection methods include polymerase chain reaction,⁵⁻⁷ culture and colony counting,^{8, 9} and immunological detection.^{10, 11} The polymerase chain reaction method can produce detection results in 5-24 hours, however that time does not include any previous enrichment steps. Culture and colony counting can take up to 16 days to get a positive result. Immunological detection can provide results within several hours, however it has low sensitivity compared to other methods. We aim to develop

a facile detection system that can positively detect low concentrations of pathogens utilizing a colorimetric sensor.

We envision a multistep detection system that employs PANI as the colorimetric sensor. Step 1 involves capturing pathogens from a food source using a fibrous support. Step 2 then entails exposing the fibrous support to a solution containing pathogen detection antibodies conjugated with horseradish peroxidase. Finally, Step 3 requires exposing the fibrous support to a dispersion containing PANI and hydrogen peroxide (H_2O_2). If pathogens are present on the fibrous support from Step 1, the fibrous support will also contain horseradish peroxidase from Step 2. Exposing the fibrous support containing pathogens (and horseradish peroxidase) to a PANI/ H_2O_2 dispersion will cause the PANI to change colors,¹² indicating the presence of pathogens.

1.1.2 Chemical warfare agent detection

Chemical warfare agents (CWA) remain a viable threat to civilian and military personnel, and therefore the detection of CWAs has been the focus of scientific research.¹³ There are several classifications of CWAs, including blister agents, choking agents, blood agents, and nerve agents. Sulfur mustard, commonly referred to as mustard gas, is a common CWA causing severe blistering when it contacts skin. Choking agents are a class of gases that are toxic to the lungs when inhaled. Some common choking agents include chlorine gas and phosgene gas. Blood agents are chemical asphyxiants that interfere with oxygen transport at the cellular level causing tissue hypoxia and lactic acidosis. A common blood agent is hydrogen cyanide. Finally, nerve agents are organophosphorus compounds that

inhibit the enzyme acetylcholinesterase, resulting in an accumulation of acetylcholine causing end-organ overstimulation. Common nerve agents include Sarin and VX.¹⁴

Due to the lethality and persistence of some CWAs, particularly the nerve agents, accurate and rapid detection methods are necessary. Some detection methods discussed in the literature include detecting dimethyl methylphosphonate (DMMP), a stimulant to Sarin, using a tin dioxide based gas sensor,¹⁵ coating a transducer with a thin polymer film that displays specificity to certain CWAs,¹³ and the fabrication of multiwalled nanotubes-polymer composites to discriminate between chemical toxic agents.¹⁶

Current detection methods in practice, particularly in the military, include placing chemical alarms in areas where a chemical attack is expected, scanning an area with a hand-held chemical agent detector, or testing unknown liquids in an area with special paper.¹⁷ Figure 1.1 shows examples of some equipment currently in use by the military for CWA detection. These methods either are reactive in nature, do not allow for rapid detection if personnel are conducting a mission in an area and are attacked, or require personnel to carry additional equipment. The development of a detection system that allows for quick and accurate detection, while allowing personnel to continue their mission without additional equipment, would be ideal. To further improve CWA detection, we propose to develop a detector that comprises a system of fiber mats for potential integration into military apparel.

1.1.3 Polyaniline

Over the last couple of decades, PANI has been the target of a significant amount of research due to its electrical and optical properties.¹⁸ PANI is of interest because it is environmentally stable, inexpensive and simple to polymerize, and can exist in several

oxidation states that provide its inherent conductive behavior. PANI can be polymerized via several methods, including electrochemical polymerization, chemical oxidative polymerization, and interfacial polymerization. Electrochemical polymerization is conducted in a conventional three-electrode cell containing a strong acid. Aniline is added to the acid solution and the electrode is cycled in the potential range -0.2 V to +0.8 V to obtain PANI films.¹⁹ Chemical oxidative polymerization utilizes two solutions; 1) an aniline in acid solution and 2) an aqueous oxidant solution, usually ammonium persulfate. The oxidant solution is added to the aniline solution, forming PANI.¹⁸ Interfacial polymerization also requires two solutions. The first solution consists of aniline in an organic solvent, such as dichloromethane. The second solution consists of an aqueous oxidant solution. The less dense solution is poured onto the more dense solution. For example, the oxidant solution would be poured onto the dichloromethane solution. PANI forms at the interface between the organic and aqueous phases.²⁰

As polymerized, PANI exists in an emeraldine salt (ES) form, also known as “doped” or “protonated” PANI, and is green in color. PANI’s highest conductivity state is in the ES form, exhibiting a conductivity of $8 \Omega^{-1}\text{cm}^{-1}$ as a solid dry film, increasing to $120 \Omega^{-1}\text{cm}^{-1}$ in a hydrofluoric medium.²¹ The oxidation states of PANI can be changed chemically via acid/base reactions and/or oxidation/reduction reactions. Figure 1.2 shows the various forms of PANI and the processes required to achieve the forms, as proposed by Stejskal and Kratochvil.²² As can be seen in Figure 1.2, each oxidation state is associated with a color. What is not as clear, however, is that conductivity changes with each oxidation state. The blue emeraldine base, the violet permigraniline base, and the colorless leucoemeraldine are

not conductive. The blue protonated pernigraniline is conductive; however it is less conductive than the green protonated emeraldine. Several groups have utilized these properties of PANI for sensor applications. Hu, et al developed an optochemical ammonia (NH₃) gas sensor from semiconductor PANI films.²³ Films were cast on glass slides and polymethyl methacrylate substrates and then exposed to various concentrations of NH₃ gas in order to determine adsorption kinetics of the gas with PANI. Dhawan, et al utilized conducting PANI as a sensor material for aqueous ammonia by capitalizing on the electrical properties of PANI.²⁴ They adsorbed PANI to insulating fibers, such as wool, to form conductive fibers. Exposing the now conductive fibers to aqueous ammonia caused a reduction in the conductivity of the fibers due to the transition of PANI from the conductive oxidation state to the insulated oxidation state. Collins, et al utilized polymer-coated fabrics for chemical sensing of ammonia gas and nitrogen dioxide gas by weaving PET or nylon threads coated with PANI into a fabric mesh.²⁵ They measured the resistivity changes of the PANI coated fibers from exposure to the toxic gases.

Despite the quantity of research dedicated to PANI and its sensing abilities, we have not found any research pertaining to chemically grafting PANI to polydimethylsiloxane. There is research on grafting PANI to polypropylene through various methods, however there is no research on grafting PANI through use of the silane coupling agent, 3-(phenylaminopropyl)trimethoxysilane. With this in mind, we intend to use 3-(phenylaminopropyl)trimethoxysilane as a coupling agent to graft PANI to polydimethylsiloxane and polypropylene, and to explore the color change rates of the two substrates grafted with PANI.

All the research mentioned thus far has used either the electrical or optical properties of PANI for sensor applications, focusing on the acid-base reaction or the reduction-oxidation reactions to change PANI from the green protonated emeraldine (conducting) form to the blue emeraldine base (non-conducting) form. A key capability of PANI that makes it so desirable in sensor applications is that the reactions are reversible. For example, after exposure to a basic vapor, such as NH_3 , the sensor can be “reset” by exposing the sensor to an acid.

1.2 Research goals and thesis organization

In this thesis, we investigate the use of PANI as a colorimetric sensor in a pathogen detection system and a chemical warfare agent detection system. In Chapter 2, we provide an overview of the detection system, and then focus on the sensor part consisting of a solution of PANI and hydrogen peroxide (H_2O_2). Above a certain concentration, hydrogen peroxide induces color change of PANI through an oxidation-reduction reaction. Below that concentration, hydrogen peroxide can still cause a color change when exposed to horseradish peroxidase. Our sensor is based on that reaction. We want to establish the optimum reaction and sensor conditions to maximize the rate of color change while lowering the sensor detection limit. We investigate the effects of several reaction conditions on the optical properties of PANI. After polymerizing PANI, we examine the effects of H_2O_2 concentration, pH, temperature, and constant agitation on the sensor system.

In Chapter 3, our goal is to graft PANI to two substrates, polydimethylsiloxane (PDMS) and polypropylene (PP), using a silane coupling agent, 3-(phenylaminopropyl)trimethoxysilane, and then compare the response times for color change

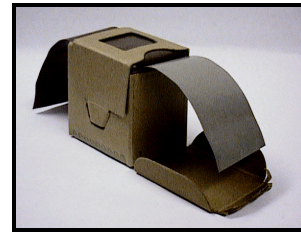
when exposed to various vapors. We are using PP because it is a common nonwoven and we chose to use PDMS because it is a flexible material known to have fast response rates to changes in the chemical environment. Additionally, the two substrates have different molecular mobility, as evident in their significantly different glass transition temperatures, and we will examine which of these two polymers provides a faster response rate when exposed various stimuli. In the chapter, we discuss modifying the surfaces of the substrates in preparation for silylation with the silane coupling agent, conducting the silylation reaction, and grafting PANI to the substrates.



(a)



(b)



(c)

Figure 1.1 Common military chemical warfare agent detectors. (a) M22 Chemical Agent Alarm;²⁶ (b) Improved Chemical Agent Monitor;²⁷ (c) M9 paper²⁸

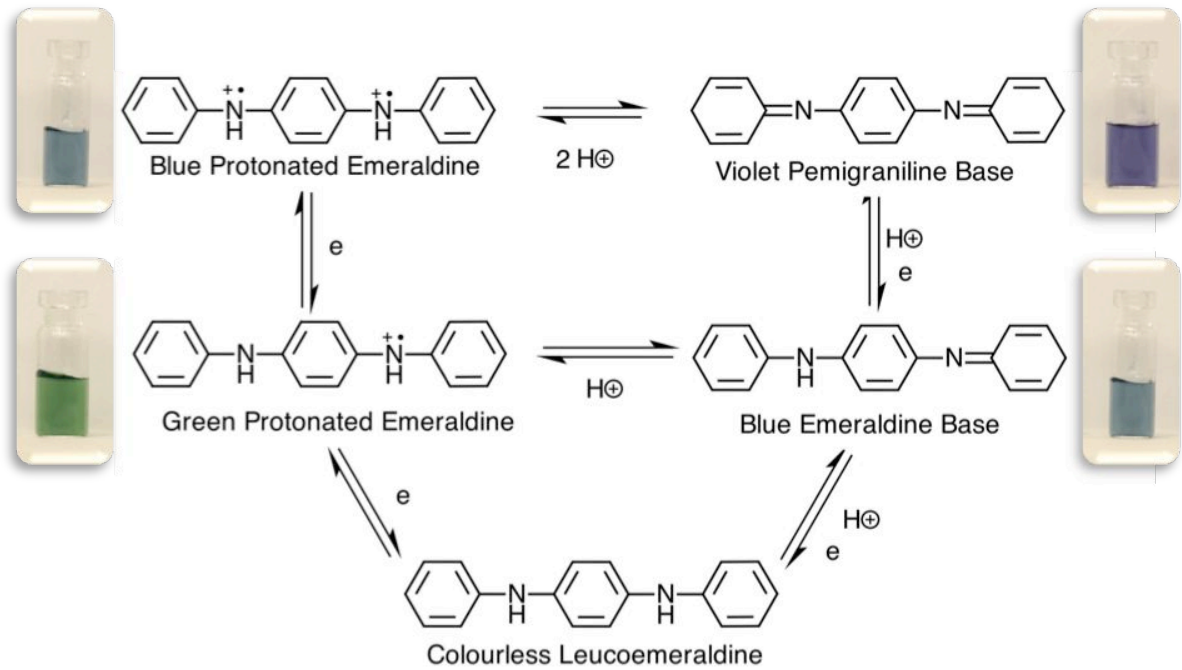


Figure 1.2 Various oxidation states of PANI, colors associated with the oxidation states, and the chemical routes that lead to each oxidation state.

REFERENCES

- (1) Statistics from *Center for Disease Control (CDC) Estimates of Foodborne Illness in the United States: CDC 2011 Estimates*, February 2011, <http://www.cdc.gov/foodborneburden/>.
- (2) Smith, K.; Hurst, C.; Moeller, R.; Skelton, H.; Sidell, F. Sulfur Mustard - its Continuing Threat as a Chemical Warfare Agent, the Cutaneous Lesions Induced, Progress in Understanding its Mechanism of Action, its Long-Term Health-Effects, and New Developments for Protection and Therapy. *J. Am. Acad. Dermatol.* **1995**, *32*, 765-776.
- (3) Szinicz, L. History of chemical and biological warfare agents. *Toxicology* **2005**, *214*, 167-181.
- (4) Mika, O. J.; Fiserova, L. Brief overview of chemical terrorism and its consequences. *Toxin Rev.* **2011**, *30*, 115-121.
- (5) Rodriguez-Lazaro, D.; D'Agostino, M.; Herrewegh, A.; Pla, M.; Cook, N.; Ikononopoulos, J. Real-time PCR-based methods for detection of *Mycobacterium avium* Subsp *paratuberculosis* in water and milk. *Int. J. Food Microbiol.* **2005**, *101*, 93-104.
- (6) Jofre, A.; Martin, B.; Garriga, M.; Hugas, M.; Pla, M.; Rodriguez-Lazaro, D.; Aymerich, T. Simultaneous detection of *Listeria monocytogenes* and *Salmonella* by multiplex PCR in cooked ham. *Food Microbiol.* **2005**, *22*, 109-115.
- (7) Deisingh, A.; Thompson, M. Strategies for the detection of *Escherichia coli* O157 : H7 in foods. *J. Appl. Microbiol.* **2004**, *96*, 419-429.
- (8) Brooks, B.; Devenish, J.; Lutze-Wallace, C.; Milnes, D.; Robertson, R.; Berlie-Surujballi, G. Evaluation of a monoclonal antibody-based enzyme-linked immunosorbent assay for detection of *Campylobacter fetus* in bovine preputial washing and vaginal mucus samples. *Vet. Microbiol.* **2004**, *103*, 77-84.
- (9) Lazcka, O.; Del Campo, F. J.; Munoz, F. X. Pathogen detection: A perspective of traditional methods and biosensors. *Biosens. Bioelectron.* **2007**, *22*, 1205-1217.
- (10) Iqbal, S.; Mayo, M.; Bruno, J.; Bronk, B.; Batt, C.; Chambers, J. A review of molecular recognition technologies for detection of biological threat agents. *Biosens. Bioelectron.* **2000**, *15*, 549-578.

- (11) Velusamy, V.; Arshak, K.; Korostynska, O.; Oliwa, K.; Adley, C. An overview of foodborne pathogen detection: In the perspective of biosensors. *Biotechnol. Adv.* **2010**, *28*, 232-254.
- (12) Piletsky, S.; Panasyuk, T.; Piletskaya, E.; Sergeeva, T.; El'skaya, A.; Pringsheim, E.; Wolfbeis, O. Polyaniline-coated microtiter plates for use in longwave optical bioassays. *Fresenius Journal of Analytical Chemistry* **2000**, *366*, 807-810.
- (13) Giordano, B. C.; Collins, G. E. Synthetic methods applied to the detection of chemical warfare nerve agents. *Current Organic Chemistry* **2007**, *11*, 255-265.
- (14) Chauhan, S.; Chauhan, S.; D'Cruz, R.; Faruqi, S.; Singh, K. K.; Varma, S.; Singh, M.; Karthik, V. Chemical warfare agents. *Environ. Toxicol. Pharmacol.* **2008**, *26*, 113-122.
- (15) Brunol, E.; Berger, F.; Fromm, A.; Planade, R. Detection of dimethyl methylphosphonate (DMMP) by tin dioxide-based gas sensor: Response curve and understanding of the reactional mechanism. *Sensors and Actuators B-Chemical* **2006**, *120*, 35-41.
- (16) Chang, C.; Yuan, C. The fabrication of a MWNTs-polymer composite chemoresistive sensor array to discriminate between chemical toxic agents. *J. Mater. Sci.* **2009**, *44*, 5485-5493.
- (17) *FM 3-11.4 Multiservice Tactics, Techniques, and Procedures for Nuclear, Biological, and Chemical (NBC) Protection*, Department of Defense, Washington, D.C., 2006.
- (18) Tzou, K.; Gregory, R. V. Kinetic-Study of the Chemical Polymerization of Aniline in Aqueous-Solutions. *Synth. Met.* **1992**, *47*, 267-277.
- (19) Wang, B.; Tang, J.; Wang, F. The Effect of Anions of Supporting Electrolyte on the Electrochemical Polymerization of Aniline and the Properties of Polyaniline. *Synth. Met.* **1986**, *13*, 329-334.
- (20) Huang, J. X.; Kaner, R. B. A general chemical route to polyaniline nanofibers. *J. Am. Chem. Soc.* **2004**, *126*, 851-855.
- (21) Genies, E.; Hany, P.; Lapkowski, M.; Santier, C.; Olmedo, L. In situ Conductivity and Photoconductivity Measurements of Polyaniline Films. *Synth. Met.* **1988**, *25*, 29-37.
- (22) Stejskal, J.; Kratochvil, P.; Jenkins, A. D. The formation of polyaniline and the nature of its structures. *Polymer* **1996**, *37*, 367-369.

- (23) Hu, H.; Trejo, M.; Nicho, M. E.; Saniger, J. M.; Garcia-Valenzuela, A. Adsorption kinetics of optochemical NH₃ gas sensing with semiconductor polyaniline films. *Sensors and Actuators B-Chemical* **2002**, *82*, 14-23.
- (24) Dhawan, S. K.; Kumar, D.; Ram, M. K.; Chandra, S.; Trivedi, D. C. Application of conducting polyaniline as sensor material for ammonia. *Sensors and Actuators B-Chemical* **1997**, *40*, 99-103.
- (25) Collins, G. E.; Buckley, L. J. Conductive polymer-coated fabrics for chemical sensing. *Synth. Met.* **1996**, *78*, 93-101.
- (26) <http://www.fas.org/man/dod-101/sys/land/m22-acada2.jpg>
- (27) <http://www.globalsecurity.org/military/systems/ground/images/nbccam1.jpg>
- (28) http://www.innotechproductsltd.com/images/stories/M_9_Paper.gif

CHAPTER 2: Dispersion Based Sensor

2.1 Introduction

The frequency of foodborne pathogen illnesses in the United States has prompted a need for a facile detection system.¹ Current detection methods can range from several hours²⁻⁴ to several days^{5, 6} for detection of a pathogen, not including additional time to prepare the sample for testing. Food supply companies have a desire for fast detecting systems for quality control of their products. Potential quality control uses of a foodborne pathogen detection system include quality testing of food immediately prior to packing and shipping and also as a random quality control check of products in storage or at stores. Prior to shipment, food products could be tested to ensure contaminated food is not being shipped to stores. A fast acting detector is necessary to facilitate the quick shipment of food to maximize freshness of the food at the store. Food supply companies do not want to wait several days to ship food while they wait for testing to determine if their food is contaminated. A detection system providing quick detection of foodborne pathogens potentially could prevent pathogen outbreaks, such as salmonella outbreaks from food supplies. After shipment of food products, companies could use a pathogen detection system to test food that is already on the shelves as a preventative measure, or to quickly test food if there is a reported case of an illness attributed to a foodborne pathogen. Quick response detection systems would allow for notification of a positive result in a timely manner, facilitating the timely removal of the contaminated food stocks from the shelves.

To this end, we aim to develop a dispersion based colorimetric sensor using polyaniline (PANI) polymerized via interfacial polymerization, hydrogen peroxide (H_2O_2), and horseradish peroxidase (HRP).

2.1.1 Detection system overview

Figure 2.1 provides a simplified graphical depiction of a proposed pathogen detection system, consisting of several steps: (a) Antibodies are immobilized on a fiber mat, creating a platform for the capture of a pathogen. The antibodies on the mat will capture a pathogen from a food sample. (b) This mat is exposed to a food sample, either by rubbing the food sample with the mat or by dipping the mat in a liquid, such as juice. (c) If a pathogen is present on the sample, the antibodies on the mat will grab the pathogen, and the mat now has foodborne pathogens on it. (d) This mat is then dipped in a solution containing antibodies conjugated with HRP. We refer to these as detection antibodies. (e) The antibodies attach to the pathogen, resulting in the mat having HRP on it. (f) The mat is then dipped in a solution consisting of PANI and H_2O_2 . The PANI solution will change colors due to the HRP on the mat catalyzing the oxidation of PANI by H_2O_2 .

This work focuses on the sensor section (see Figure 2.1f) of the pathogen detection system. The primary goal of this work is to assess PANI as a colorimetric sensor for the detection of HRP. First, we examine if PANI dispersed in a hydrogen peroxide solution changes color in the presence of HRP. Once we determine that PANI dispersed in H_2O_2 changes color after the addition of HRP, we examine several detection conditions to determine the HRP detection limit of the sensor. We do this because in our detection system HRP is only present when pathogens are present. If we are able to detect a low concentration

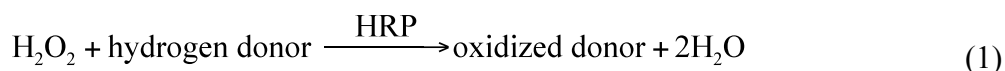
of HRP, then we are able to detect a low concentration of pathogens. To evaluate the detection limit of our sensor, we examine the effect of temperature, pH, and agitation on HRP detection.

2.1.2 Horseradish peroxidase and hydrogen peroxide

Horseradish peroxidase is a monomeric heme-containing enzyme that catalyzes the oxidation of a variety of organic compounds by hydrogen peroxide.^{7, 8} A heme is an iron containing prosthetic group of an enzyme. Heme has the redox potential for several catalytic reactions due to its ability to collect electrons. This ability allows heme-containing enzymes to catalyze the oxidation of organic compounds by activating H₂O₂.⁹

HRP and hydrogen peroxide are frequently used in chemiluminescent assays and chromogenic assays.¹⁰⁻¹² The chemiluminescent and chromogenic assays emit light and color, respectively, when oxidized. In both these processes, HRP conjugates target specific molecules and are then exposed to chemiluminescent or chromogenic substrates in the presence of H₂O₂. HRP catalyzes the oxidation of the substrates by H₂O₂, causing the substrates to emit light or color. In our sensor, PANI is akin to the previously mentioned chemiluminescent and chromogenic substrates. PANI is dispersed in H₂O₂ and we expect it to be oxidized when HRP is added, thus causing a color change.

Although hydrogen peroxide is a strong oxidizer, it will not oxidize PANI in small enough concentrations. However, in the presence of HRP, hydrogen peroxide will oxidize PANI according to the following reaction:



where PANI is assumed to act as the hydrogen donor.¹³

In our proposed detection system, HRP is conjugated to an antibody with an affinity for a foodborne pathogen. If a pathogen is present on the fiber mat, HRP will be on the fiber mat due to the HRP conjugated antibodies binding with the pathogen. The fiber mat will be placed in a solution consisting of PANI and H₂O₂. If HRP is present on the mat, the HRP will catalyze the oxidation of PANI via H₂O₂, according to Equation (1), indicating the presence of a foodborne pathogen.

2.1.3 Polyaniline

Polyaniline is a conducting polymer that achieves its conductivity from its multiple oxidation states. In addition to each oxidation state affecting the conductivity of PANI, each oxidation state is associated with a color. Transitions between different oxidation states occurs via acid-base reactions and oxidation-reduction reactions.¹⁴ Researchers have focused on both the optical¹⁵⁻¹⁷ and electrical¹⁷⁻²⁰ properties of PANI when developing various sensor systems. PANI has seen success in research as a sensor platform for the detection of several gases,^{21,22} including ammonia^{23,24} and nitrogen dioxide.²³ Many sensors based on PANI have utilized PANI in the solid state, such as a films^{22, 24, 25} or fibers.^{17, 19, 26}

We intend to concentrate on the oxidation-reduction route to transition from one PANI oxidation state to another. Our sensor will use PANI in a dispersion with hydrogen peroxide to capitalize on the HRP catalyzed oxidation of PANI by H₂O₂, similar to that of other systems built around chromogenic substrates, HRP, and H₂O₂.

2.2 Materials and Methods

2.2.1 Materials

Aniline hydrochloride, ammonium persulfate (APS), dichloromethane (DCM), and hydrochloric acid (HCl) used in the polymerization of polyaniline (PANI) were obtained

from Sigma-Aldrich. Hydrogen peroxide (35% w/w) and horseradish peroxidase (type II, 150-250 units/mg) were obtained from Sigma-Aldrich. Deionized (DI) water was produced via a Dracor filter system from Dracor Water Systems.

2.2.2 Polyaniline polymerization

PANI was synthesized via interfacial polymerization.²⁷ The organic phase consisted of 0.32 mol of the monomer, aniline hydrochloride, dissolved in 1 liter of DCM. Due to some non-dissolved aniline, the organic phase of the solution was a grey-green color. The clear aqueous phase comprised of 0.08 mol of the oxidant (ammonium persulfate) dissolved in 1 liter of 1 M HCl. Since the organic phase has a higher density than the aqueous phase, it served as the bottom phase for the interfacial polymerization. The organic phase was poured into a 2 L jar and placed in an ice bath for pre-cooling. The aqueous phase was slowly poured into the 2 L jar via a funnel directed towards the side of the jar to prevent mixing of the phases. The reaction proceeded overnight. Figure 2.2 graphically depicts the interfacial polymerization of PANI. Once the organic phase turns an amber color, the reaction is complete. The aqueous phase, containing PANI, is separated from the organic phase via pipette.

2.2.3 Purification of PANI

PANI was purified via dialysis using Fisherbrand dialysis tubing obtained from Fisher Scientific. The dialysis tubing had a molecular weight cut-off (MWCO) of 12,000-14,000 Daltons and a flat width of 10 mm. The dialysis tubing is filled with PANI and placed in a 3 L beaker filled with DI water. The dialysis tube is filled with PANI, placed in three liters of DI water for two hours. At this point, the DI water was flushed to facilitate

continued diffusion of PANI impurities from dialysis tubing to the water in the beaker. This procedure was repeated at a minimum two more times in a 24-hour window. After completion of the purification, the PANI was collected from the dialysis tubing and placed in a jar for future use.

2.2.4 Scanning Electron Microscopy (SEM)

SEM was conducted on FEI XL30 Field Emission SEM using a TLD detector at a working distance of 5.8 mm with an accelerating voltage of 5 kV. The magnification of the SEM images ranged from 2500x to 160000x.

2.2.5 Ultraviolet-Visible Spectroscopy (UV-VIS)

UV-VIS spectra of the PANI solutions were taken using a JASCO V-550 UV-VIS spectrophotometer. Spectra were determined by measuring a reference and the sample simultaneously. Samples were placed in 2 mL polystyrene cuvettes obtained from VWR. Spectra peaks were analyzed using the Spectra Manager software provided by the manufacturer.

2.3 Results and Discussion

2.3.1 Polyaniline polymerization

Figure 2.3 shows the progress of the interfacial polymerization of PANI. Immediately upon pouring the aqueous phase on to the organic phase, a color change was observed in the aqueous phase, indicating the reaction was occurring, as shown in Figure 2.3(b). When initially formed, the PANI was violet in color and iridescence was observed in the aqueous phase. After an hour, a thin amber color was observed at the interface in the organic phase. Figure 2.3(c) shows that after adding all of the oxidant solution, the aqueous phase was completely green with polymerized PANI. After allowing the reaction to run

overnight, it appeared to be complete due to the organic phase being dark amber in color and the aqueous phase being dark green in color, as seen in Figure 2.3(d). The amber colored organic phase and the green aqueous phase were indicators the reaction was complete.²⁷

When the aqueous phase was poured on to the organic phase, the APS oxidant oxidized the aniline monomer forming an aniline cation radical as illustrated in Figure 2.4(a). The aniline cation radical formed one of its three resonance structures (see Figure 2.4(b)), most likely using the center form for the formation of PANI due to its lack of steric hindrance. The aniline cation radical then reacted with its resonance form, producing a dimer (see Figure 2.4(c)). Through a series of hydrogen losses and rearrangement, the dimer polymerized to form para-aminodiphenylamine (PADPA) (see Figure 2.4(d)). PADPA was then oxidized, forming a dimer cation, which reacted with either an aniline monomer cation or another dimer cation, forming a trimer or tetramer. This process continued until completion of the polymerization reaction.^{14, 28}

Following completion of the PANI polymerization, the aqueous phase was separated from the organic phase via pipette. The PANI in the aqueous phase was purified using dialysis tubing and monitored by the changing pH of the aqueous media (starting pH was 7.28). Once the DI water receiver reached a pH of 4.88, sufficient acidic impurities had diffused across the dialysis membrane completing one purification cycle. The acidic impurities were expected because the aqueous phase was in 1 M HCl and H⁺ ions were released during the polymerization of PANI.¹⁴ Subsequent DI water changes resulted in smaller pH changes over longer periods of time until a pH change plateau indicated the dialysis completion. The final purified product was dark green.

In order to analytically verify the observed color of the PANI, UV-VIS spectroscopy was conducted for polymerized PANI through determination of the minimum absorbance wavelength to correlate with wavelength of the color that is visually seen. For measurement in the UV-VIS spectrometer, the purified PANI was diluted with DI water to avoid oversaturating the spectrometer. Figure 2.5 shows the UV-VIS spectra for the polymerized PANI in DI water where the minimum absorbance wavelength was 493.5 nm. This value is consistent with the green region wavelength in the visible light spectrum. Scanning electron microscopy was performed on samples of the purified PANI. Figure 2.6 shows the SEM images from 2500x magnification to 80000x magnification. The images at higher magnifications show the formation of a network of nanofibrils and a porous medium. The porous nature of the PANI could allow for better mass transport of the oxidizing agent, facilitating the oxidation and color change of PANI. The images were in agreement with those obtained by Huang, et al during their investigation of polymerization conditions on the interfacial polymerization of PANI.²⁷

2.3.2 Determining optimum H₂O₂ concentration

Our sensor is based on HRP catalyzing the oxidation of PANI by H₂O₂. When PANI is oxidized, it changes color from green to blue to violet, causing a decrease in the minimum absorbance wavelength. Hydrogen peroxide is a strong oxidizer and in high enough concentrations, will oxidize PANI without the addition of HRP. If the concentration of H₂O₂ is too high, it will fully oxidize PANI to the violet pemigraniline base form. Once PANI is in the violet pemigraniline base form, the addition of HRP will not cause any further color change as the PANI cannot be further oxidized and the PANI is already at the end of the

visible spectrum, making it impossible to observe any further color changes. Therefore, we examined the effect of various concentrations of H_2O_2 on PANI, with a goal of determining the highest concentration of hydrogen peroxide that will not cause the oxidation of PANI without the presence of HRP. The oxidation of PANI was determined by a shift (i.e., decrease) in the minimum absorbance wavelength, as a decrease in the minimum absorbance wavelength indicates a color change from green (the color of polymerized PANI) to blue to violet.

Figure 2.7 shows the effect of different concentrations of H_2O_2 (0.05 mM, 0.125 mM, 0.25 mM, and 0.50 mM) on PANI solutions. The highest H_2O_2 concentration (0.50 mM) has a significant change in the minimum absorbance wavelength for the PANI solution. The significant change in minimum absorbance wavelength indicates a change in the color of the PANI, thus the oxidation state of PANI is changing. The lower concentrations of H_2O_2 resulted in little to no change in the minimum absorbance wavelength of PANI, suggesting no change in color or oxidation state was occurring.

Since the lower three concentrations (0.05 mM, 0.125 mM, and 0.25 mM) of H_2O_2 showed no change in the PANI oxidation state, we investigated the effect of varying peroxide concentration on PANI in the presence of HRP. We did this to determine which hydrogen peroxide concentration resulted in the fastest rate of color change of PANI after the addition of HRP since our sensor is based on the oxidation (color change) of PANI after the addition of HRP. Figure 2.8 shows at a higher concentration of HRP (550 nM), the concentration of H_2O_2 had little effect on the rate of color change of PANI. PANI dispersions in 0.125 mM and 0.25 mM H_2O_2 both changed color at approximately the same rate as is evident by a

similar decrease in the minimum absorbance wavelength. However, at a lower concentration of HRP (5.5 nM), 0.25 mM H₂O₂ was needed to observe a visual change in the optical properties of PANI and to observe a shift in the minimum absorbance wavelength of the PANI solution. At 0.125 mM H₂O₂ and 5.5 nM HRP, no color change was observed and there was no change in the minimum absorbance wavelength, verifying what was seen visually. As a result, an H₂O₂ concentration of 0.25 mM was used for subsequent experiments.

2.3.3 Determining optimum pH

In addition to the hydrogen peroxide concentration, the oxidation state of PANI is affected by the pH of the solution. As polymerized, PANI is in its protonated acidic state. The acid-base transition occurs at a pH between zero and one,¹⁴ therefore when the PANI solution is exposed to any pH greater than one, the oxidation state of PANI is expected to change with the associated color indication of the solution. The PANI solution accordingly changed from green to blue to purple as a function of pH. To insure the starting solution was not at the detection limits of the visible spectrum (violet is very close), we targeted a starting solution color of green or blue. Figure 2.9 shows the effect of several pH buffers on PANI. The minimum absorbance wavelength was measured each hour to determine the effect of the various pH buffers over time. The starting minimum absorbance wavelengths (time = 0) were different due to the immediate effect on PANI of increasing the pH, however all PANI solutions in each pH buffer exhibited a shift of approximately 25 nm. After six hours the minimum absorbance wavelengths began to plateau. At this point, we added H₂O₂ to observe the effects of hydrogen peroxide on PANI in the various pH buffers because our sensor

requires the presence of H₂O₂. We wanted to determine if any pH buffer/H₂O₂ solutions cause PANI to be fully oxidized, making it unusable for our sensor. The H₂O₂ was added after the minimum absorbance wavelengths plateaued so we could attribute any changes to the PANI solution to the appropriate factor. After 18 hours of exposure to 0.25 mM H₂O₂ in each pH buffer, PANI solutions in pHs ≥ 6.0 had similar minimum absorbance wavelengths, at approximately 440 nm. Solutions exhibiting a minimum absorbance wavelength near 440 nm were blue in color. Using solutions with a minimum absorbance of 440 nm was advantageous because a color change to violet would be observed at a wavelength of approximately 430 nm, requiring only a small change to the oxidation state.

In addition to utilizing pH buffers to generate PANI solutions of an advantageous color and minimum absorbance wavelength, the solutions must also optimize HRP activity. According to *Enzyme Handbook 7*, the optimum pH for HRP activity is between 6.0 and 6.5.²⁹ Based on the effects of the various pH buffers on PANI and the optimum pH for HRP activity, we used a buffer pH of 6.0 and 6.4 for the HRP detection experiments.

2.3.4 Effect of temperature on HRP detection

We determined the solution conditions for HRP detection would be for a PANI dispersion in pH 6.0 and 6.4 buffers and 0.25 mM H₂O₂. We investigated the effect of temperature on the catalytic reaction between HRP and H₂O₂ to oxidize PANI as we expect a faster reaction rate with increasing temperature. Initial experiments were done at HRP's storage temperature of 4°C with a resultant reaction rate of 1683 minutes for a detection limit of 5.5 nM HRP. In an attempt to improve the reaction rate, and potentially increase detection sensitivity, experiments were done at room temperature (approximately 22°C) and at 5°C

increments from 30°C-50°C. We did not investigate the effect of temperatures greater than 50°C because HRP is stable for only 30 minutes at 50°C and inactive at 52°C.²⁹

Figure 2.10 shows the effect of color change rate as a function of temperature. Higher temperatures resulted in a faster color change rate of PANI solutions with 0.25 mM H₂O₂ and various HRP concentrations. Figure 2.10 illustrates that at solution conditions of pH 6.4 and an HRP concentration of 5.5 nM, PANI changed color in 30 minutes at 45°C, as opposed to changing in nearly 1700 minutes at 4°C. The oxidation of PANI exhibits behavior that follows the Arrhenius equation:

$$k = Ae^{\frac{-E_a}{RT}} \quad (2)$$

where k is the rate constant, A (Arrhenius A factor) and E_a (activation energy) are constants characteristic of the reaction, R is the universal gas constant, and T is the temperature of the reaction. Equation (2) was rearranged to Equation (3) below to make it possible to solve for E_a .

$$\ln\left(\frac{k}{A}\right) = -\left(\frac{E_a}{R}\right)\left(\frac{1}{T}\right) \quad (3)$$

Plotting the natural log of color rate change as a function of inverse reaction temperature (see Figure 2.11), allows us to determine the slope from Equation (3). The activation energy is then determined by using Equation (4):

$$E_a = -R * \text{slope} \quad (4)$$

The activation energy of our reaction (HRP catalyzed oxidation of blue emeraldine base to violet pemigraniline base) was 71.9 kJ/mol for solution conditions of pH 6.4, 0.25 mM H₂O₂, and 5.5 nM HRP. Moon, et al found the activation energy of oxidizing the leucoemeraldine base to emeraldine base to be 50.4 kJ/mol when oxidized by oxygen gas at 30°C.³⁰

To insure increasing the temperature was not causing H₂O₂ to further change the oxidation state of PANI prior to the addition of HRP, we investigated the effect of increasing temperature on solutions of PANI and H₂O₂ without the presence of HRP. Figure 2.12 shows increasing temperature does not cause H₂O₂ to further oxidize PANI, prior to addition of HRP. PANI in pH 6.4 buffer and 0.25 mM H₂O₂ exhibited a decrease in minimum absorbance wavelength of only 3 nm, not enough to indicate a color change or change in oxidation state. Therefore, the increase in temperature did not cause hydrogen peroxide to oxidize the PANI, rather the addition of HRP at increased temperature caused the oxidation of PANI and improved reaction rate.

After examining the effect of temperature on the detection of HRP, we found the optimal conditions for HRP detection to be 0.25 mM H₂O₂, pH 6.0 or pH 6.4, and a solution temperature of 45°C.

2.3.5 Effect of constant agitation

During the experiments, we observed that PANI settled out of solution (see Figure 2.13). After approximately three hours, the settling was noticeable (see Figure 2.13(b)), and after being undisturbed overnight, the PANI solution had completely settled (see Figure 2.13(c)). Prior to recording absorbance measurements, we needed to shake the PANI solution to get a homogenous solution. Since our sensor is based on the HRP catalyzed

oxidation of PANI by H_2O_2 , we wanted the maximum amount of PANI to come in contact with the hydrogen peroxide to facilitate the oxidation of the PANI in solution. PANI settling to the bottom of the vial may have resulted in less PANI being available for oxidation, limiting the amount of color change observed. This does not pose a problem for high concentrations of HRP since the higher concentrations of HRP catalyzed the H_2O_2 oxidation of PANI (and resultant color change) prior to the PANI settling out of solution. However, at lower concentrations of HRP, the times for color change were slower, and the PANI would settle. We investigated the effect of constantly stirring the solution at room temperature (22°C) in an effort to keep the solution as homogenous as possible and maximizing the exposure of PANI to the HRP catalyzed H_2O_2 to facilitate the color change of PANI. Figure 2.14 shows that constant stirring of the solution resulted in color change occurring twice as fast as without stirring at HRP concentrations of 5.5 nM (Figure 2.14(a)) and 0.55 nM (Figure 2.14(b)). The effect of constant stirring was independent of pH, as we saw similar results at pH 6.0 and pH 6.4.

2.4 Conclusions and Future Work

A novel HRP detection system has been developed using PANI to detect HRP at concentrations ranging from 550 nM down to 0.55 nM using a dispersion consisting of PANI and 0.25 mM H_2O_2 . We were able to detect an HRP concentration of 0.55 nM in 40 minutes using the optimal reaction conditions of 22°C , 1.35 mM PANI, 0.25 mM H_2O_2 , pH 6.0 and pH 6.4, and maintaining the solution at constant agitation. These results were a significant improvement over our initial results of an HRP detection limit of 5.5 nM at 4°C and no limited mixing. At those conditions, the rate of color change was 1683 minutes.

Future work will involve the investigation of three more factors. First, investigation will be done on the effect of constant agitation at various temperatures. As already shown, increased temperatures result in a faster reaction rate for PANI dispersions with limited mixing. At room temperature, constant agitation increased the reaction rate. Therefore, the next step is to determine the reaction rate of the PANI/H₂O₂ dispersion in the presence of HRP at increasing temperatures without mixing limitations. The second factor for further investigation is the effect of PANI concentration as the described experiments have been conducted at a constant PANI concentration of 1.35 mM. While lower concentrations of HRP may be catalyzing the H₂O₂ oxidation of PANI, there is a chance that all of the PANI may not be getting oxidized minimizing the apparent color change. Various PANI concentrations will be investigated under constant agitation and various temperatures to insure that the level of PANI is not oversaturated for a visible color change. Finally, conjugated HRP will be investigated versus the current procedure of utilizing free HRP. As we envision the final detection system to be based on immobilized HRP, we need to insure that its efficiency is not hampered once bound to a substrate. Conjugating HRP to an antibody will mimic the effects of immobilized HRP thus this reaction scheme will be investigated under the same reaction conditions as performed for the free HRP system.

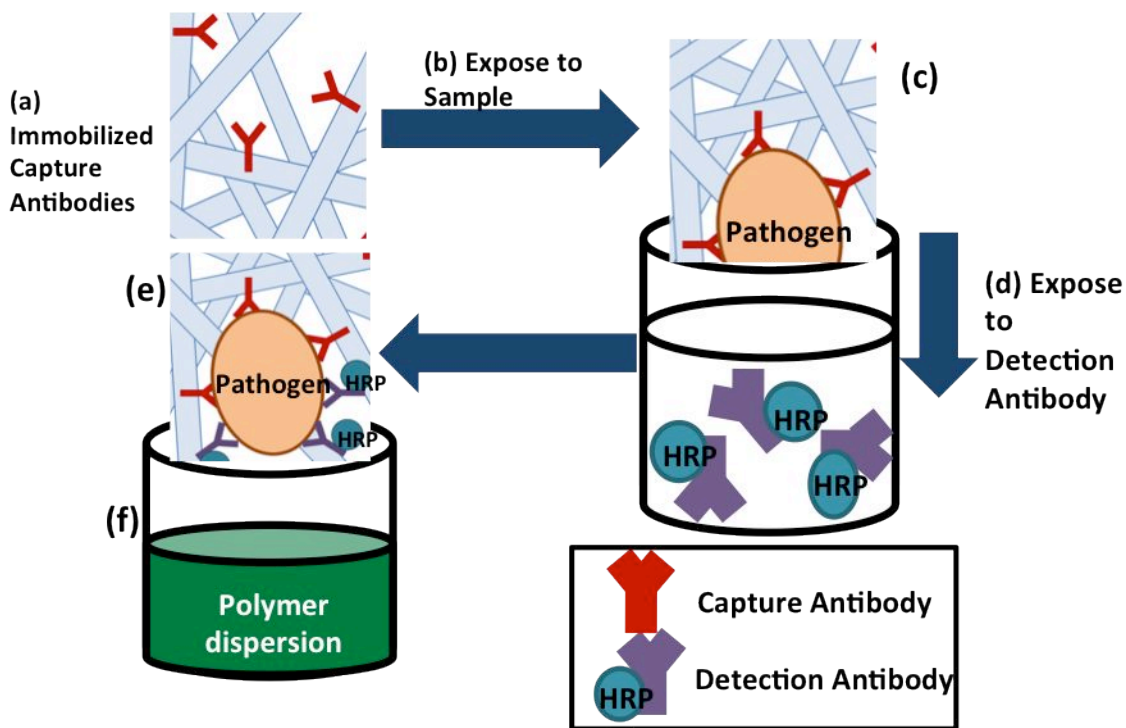


Figure 2.1 Overview of pathogen detection system. (a) Capture antibodies are immobilized on a fiber mat. (b) The mat is exposed to a sample. (c) If a pathogen is present, the capture antibodies will capture it. (d) The mat is then exposed to detection antibodies (antibodies conjugated with HRP). (e) If a pathogen is present, the detection antibodies will bind to the pathogen. (f) The mat is then placed in a PANI and H_2O_2 solution. If a pathogen is present, the HRP that is conjugated on the capture antibody that is bound to the pathogen will catalyze the oxidation of the PANI solution by H_2O_2 , causing a change in oxidation states and color of the PANI.

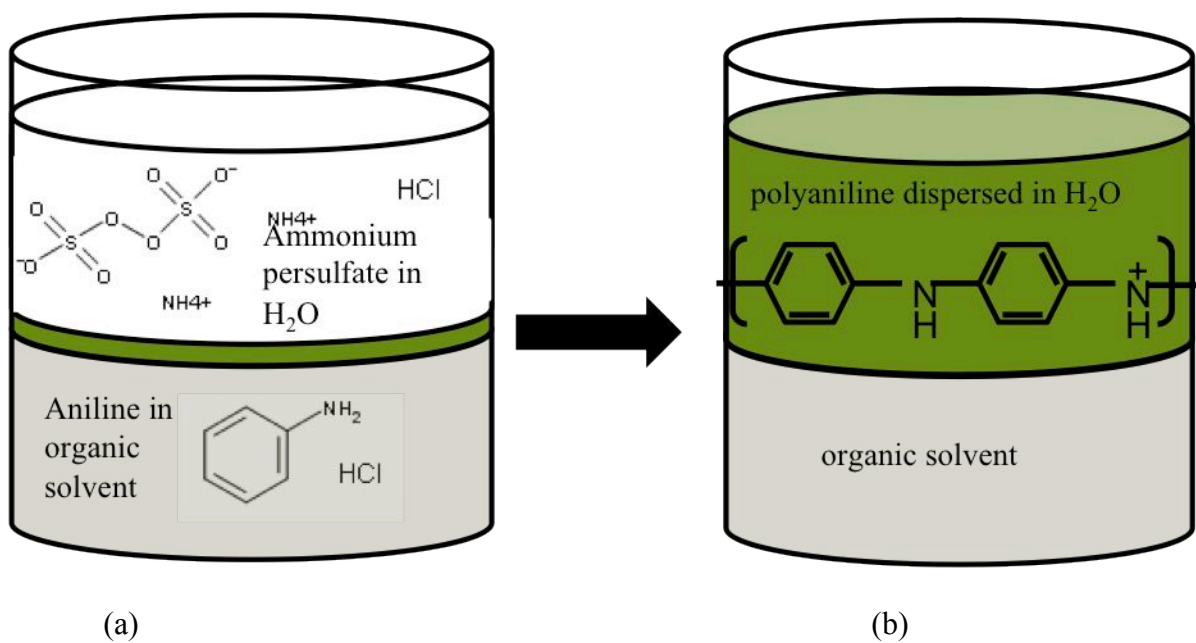


Figure 2.2 Interfacial polymerization of PANI. (a) Aniline is dissolved in the organic phase and the oxidant, ammonium persulfate, is in HCl. The aqueous oxidant solution is slowly added to the organic phase. Immediately PANI forms at the interface between the aqueous and organic phases. (b) At the completion of the reaction, PANI is dispersed in the aqueous phase and no aniline monomer remains in the organic phase.

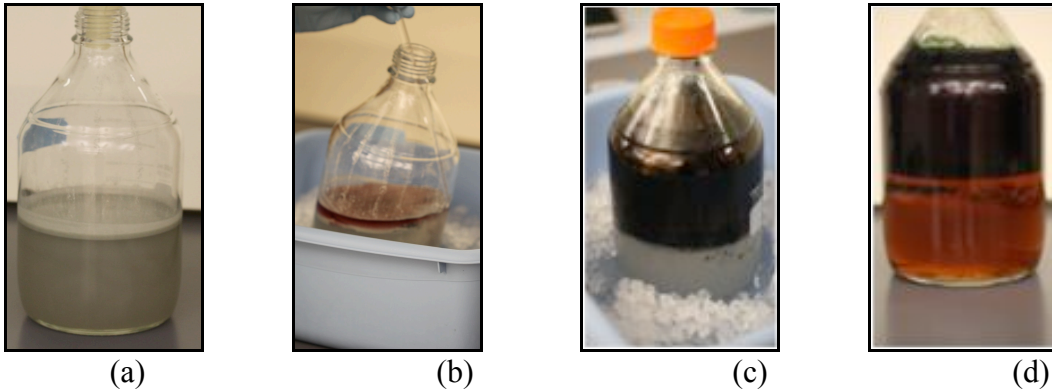


Figure 2.3 Progress of interfacial polymerization of polyaniline. (a) Aniline-hydrochloride in dichloromethane before addition of aqueous phase. (b) Addition of aqueous phase. Immediately upon contact of the aqueous phase with the organic phase, red was observed. As more aqueous phase was added, the color changed from red to blue to green. (c) Completion of addition of aqueous phase. After the aqueous phase was added, the aqueous phase was green. (d) Completion of polymerization. The organic phase was dark amber, indicating completion of the reaction. The aqueous phase was dark green.

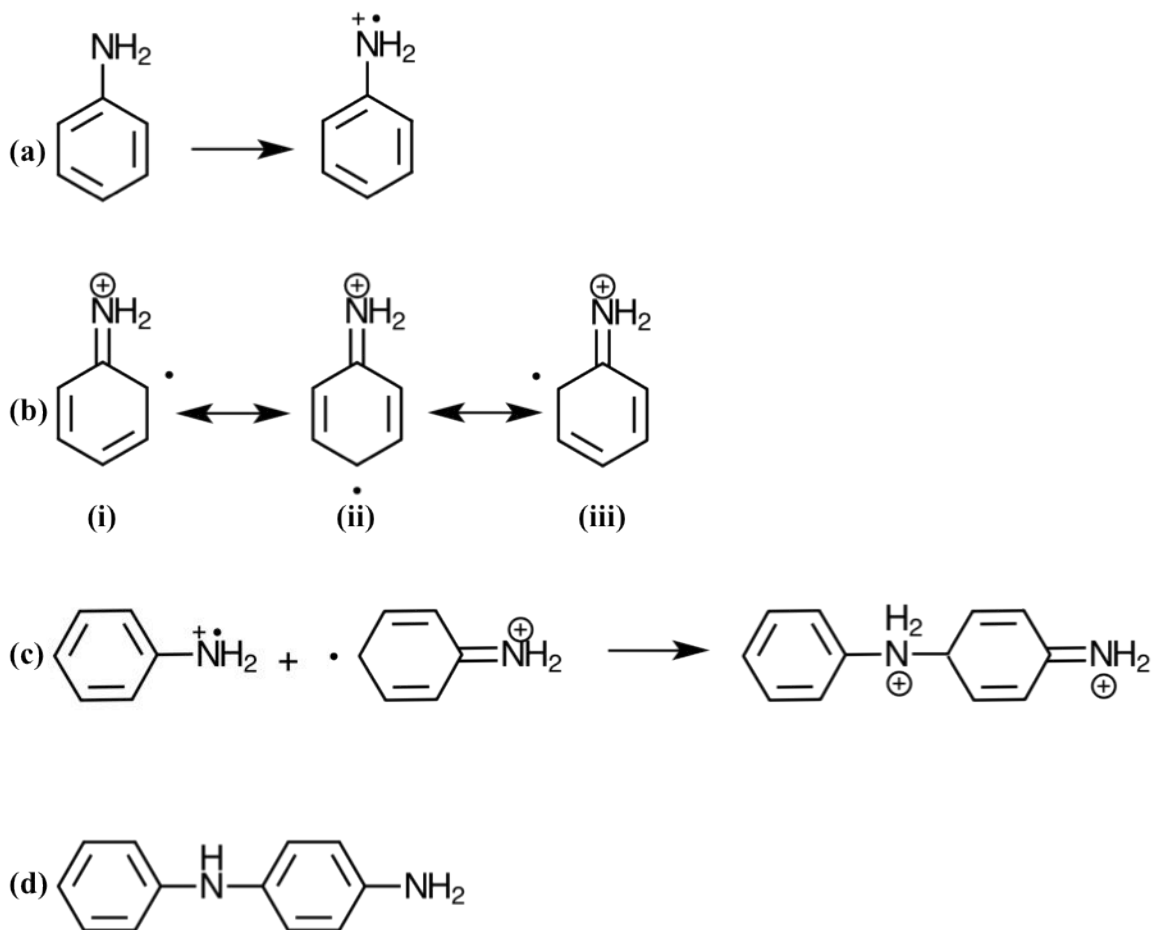


Figure 2.4 Polymerization of PANI. (a) Aniline cation radical formed when aniline monomer reacts with an oxidant to initiate the polymerization of PANI. (b) Resonance structures formed from the aniline cation radical. Form (ii) is most likely the most reactive species due to the availability of the radical. (c) The formation of a polyaniline dimer. The aniline cation radical reacts with one of the resonance structures of the cation radical, forming a dimer. (d) After the release of 2 hydrogens and rearrangement, the dimer becomes para-aminodiphenylamine (PADPA). PADPA is oxidized twice forming a radical dimer which then reacts with other radicals in solution, forming PANI.

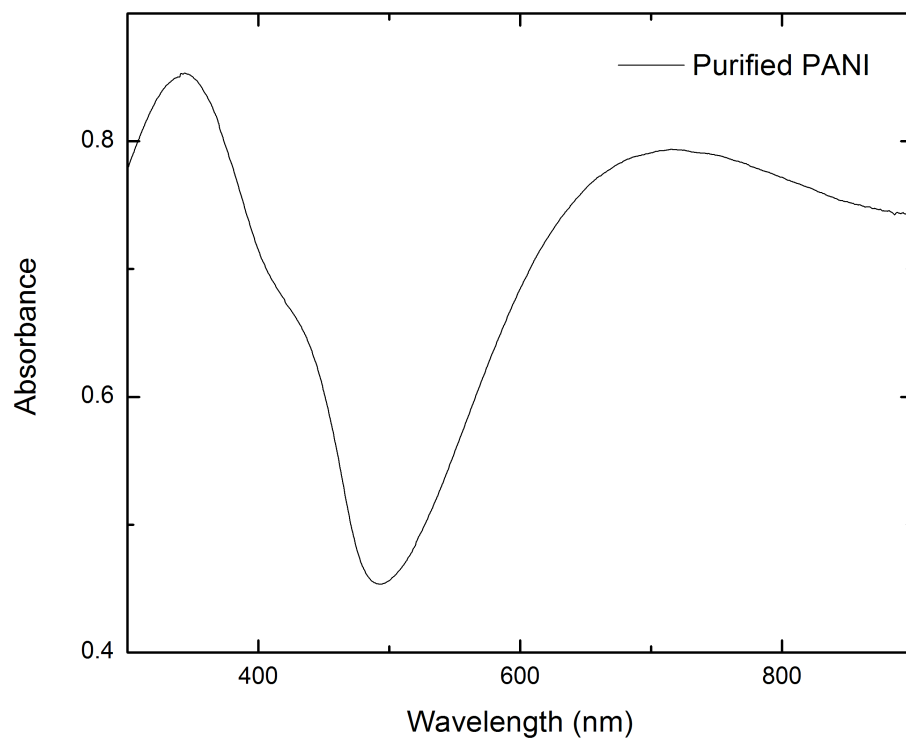


Figure 2.5 UV-VIS spectrum of PANI in DI water after interfacial polymerization. The minimum absorbance value of 493.5 nm indicated the PANI was green in color.

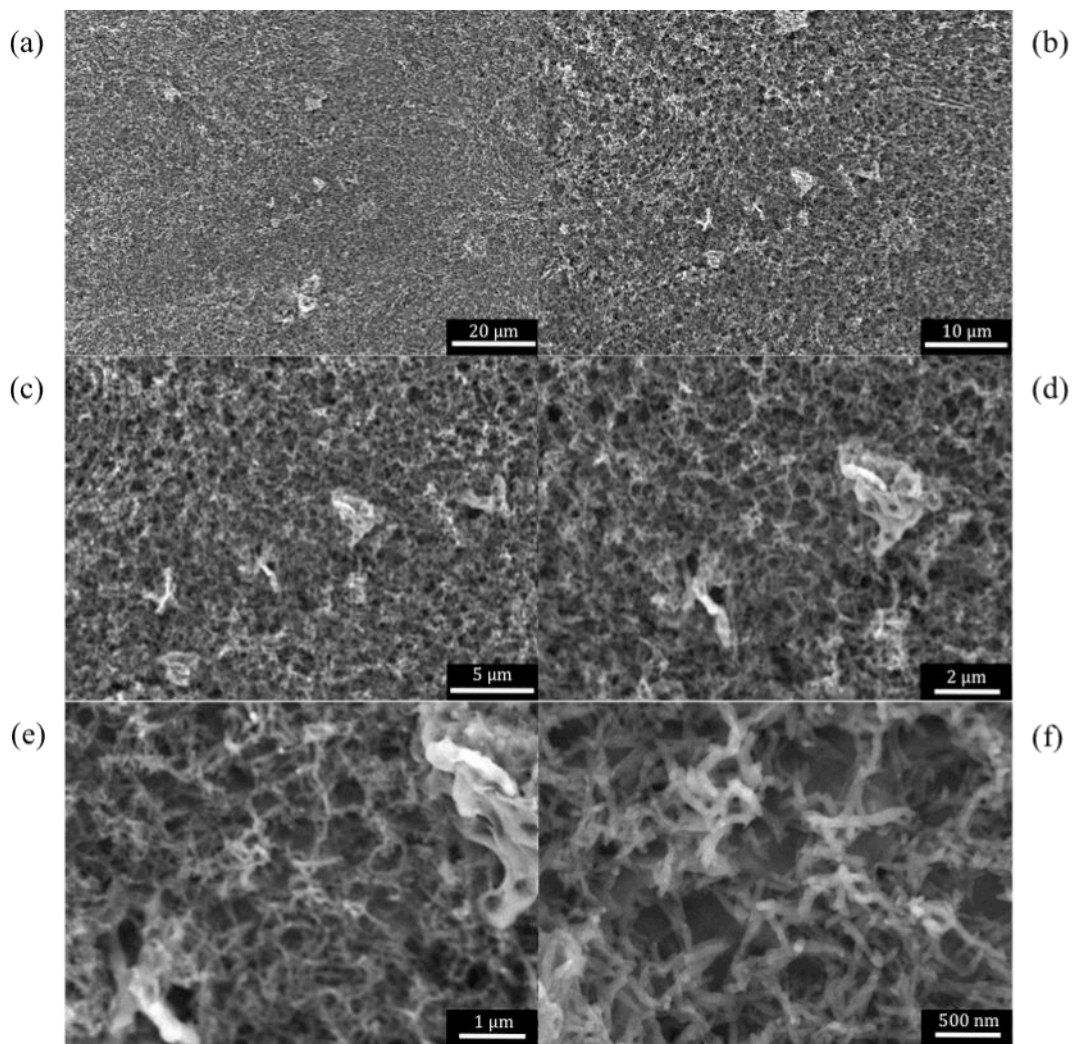


Figure 2.6 SEM micrographs of PANI. (a) 2500x magnification, (b) 5000x magnification, (c) 10000x magnification, (d) 20000x magnification, (e) 40000x magnification, (f) 80000x magnification.

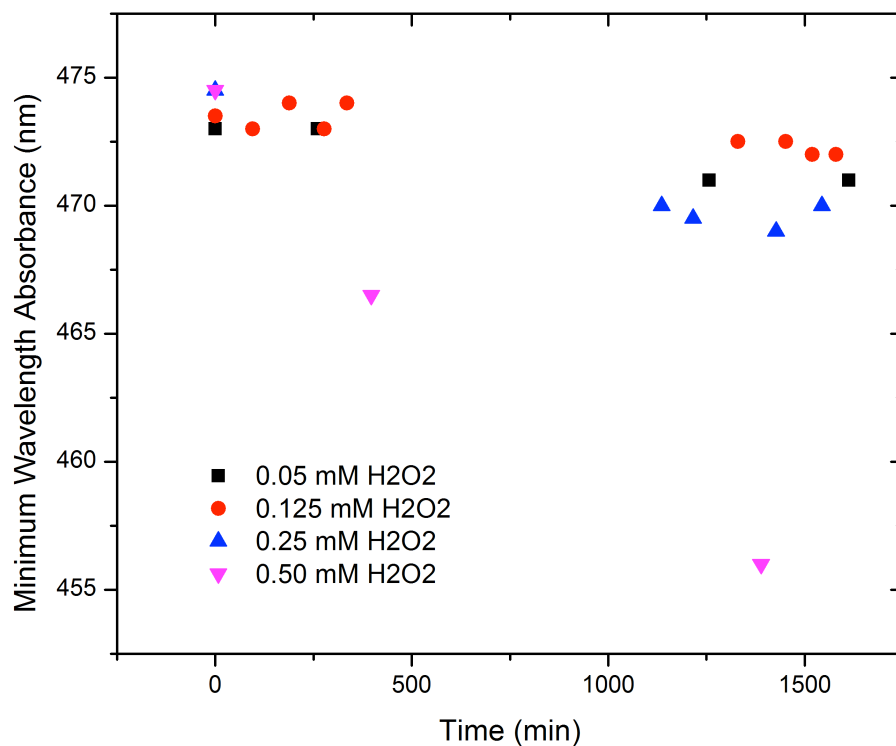


Figure 2.7 Effect of H₂O₂ concentration on PANI. After over 25 hours, H₂O₂ concentrations ≤ 0.25 mM had little to no effect on the oxidation of PANI, however PANI was being oxidized after a few hours at an H₂O₂ concentration of 0.50 mM.

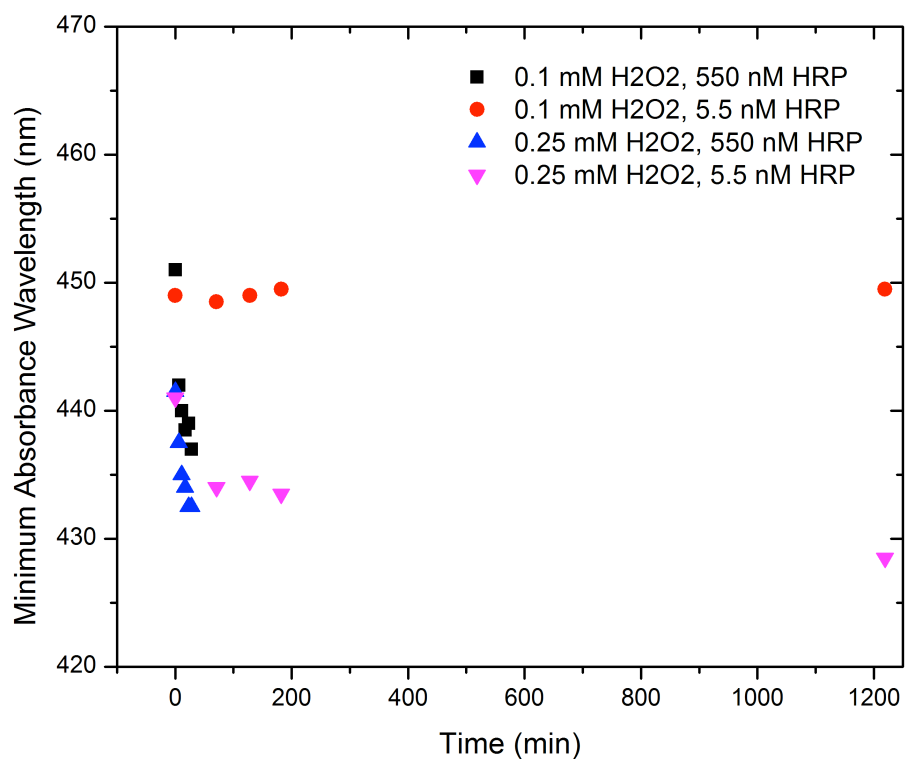


Figure 2.8 The effect of different H₂O₂ concentrations and different HRP concentrations on the oxidation of PANI. At an HRP concentration of 550 nM, PANI was oxidized regardless of the H₂O₂ concentration (black squares and blue triangles). At an HRP concentration of 5.5 nM, 0.1 mM H₂O₂ (red circle) did not oxidize PANI, however 0.25 mM H₂O₂ (inverted purple triangle) did oxidize PANI.

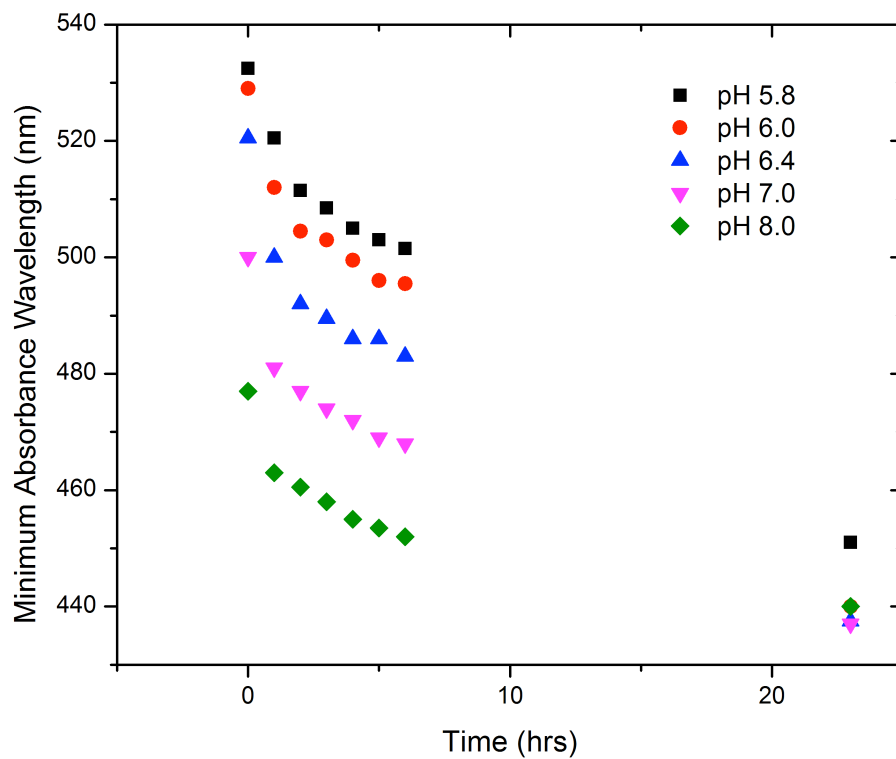


Figure 2.9 Effect of pH on PANI as a function of time. H_2O_2 was added after six hours.

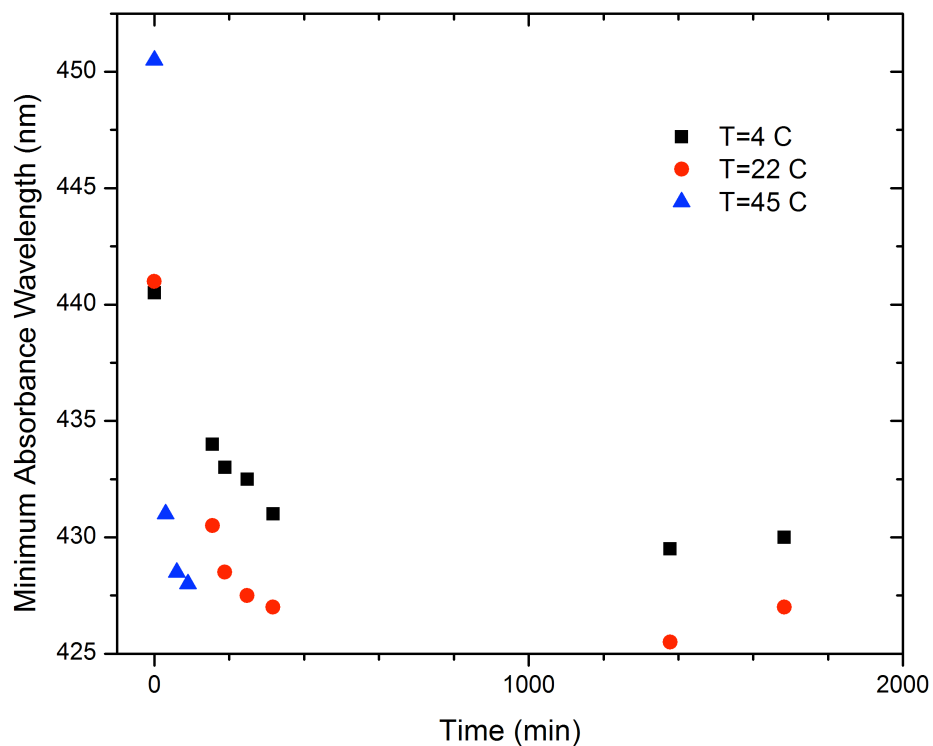


Figure 2.10 Effect of increasing temperature on rate of color change for PANI at pH 6.4, 5.5 nM HRP, 0.25 mM H₂O₂. At T=4°C, color change occurred at 1683 min. At T=22°C, color change occurred at 188 min. At T=45°C, color change occurred at 30 min.

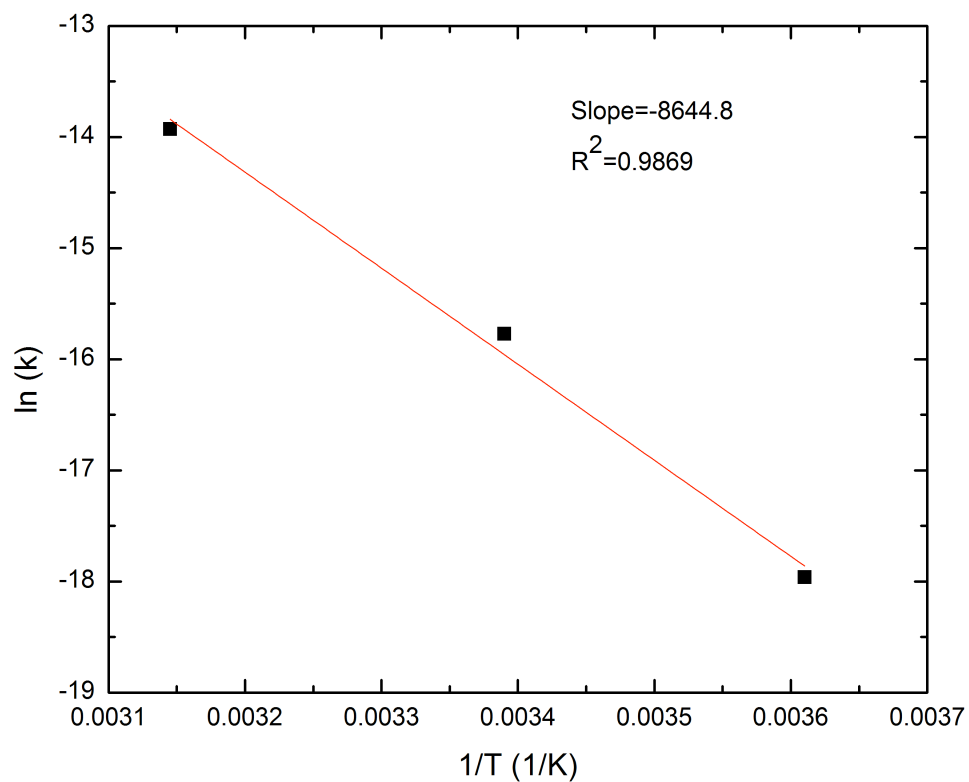


Figure 2.11 Arrhenius plot of oxidation of PANI at pH 6.4, 0.25 mM H_2O_2 , 5.5 nM HRP, and $T=4^\circ C$, $22^\circ C$, and $45^\circ C$. Using the slope of the linearly fitted line, the activation energy (E_a) was 71.9 kJ/mol.

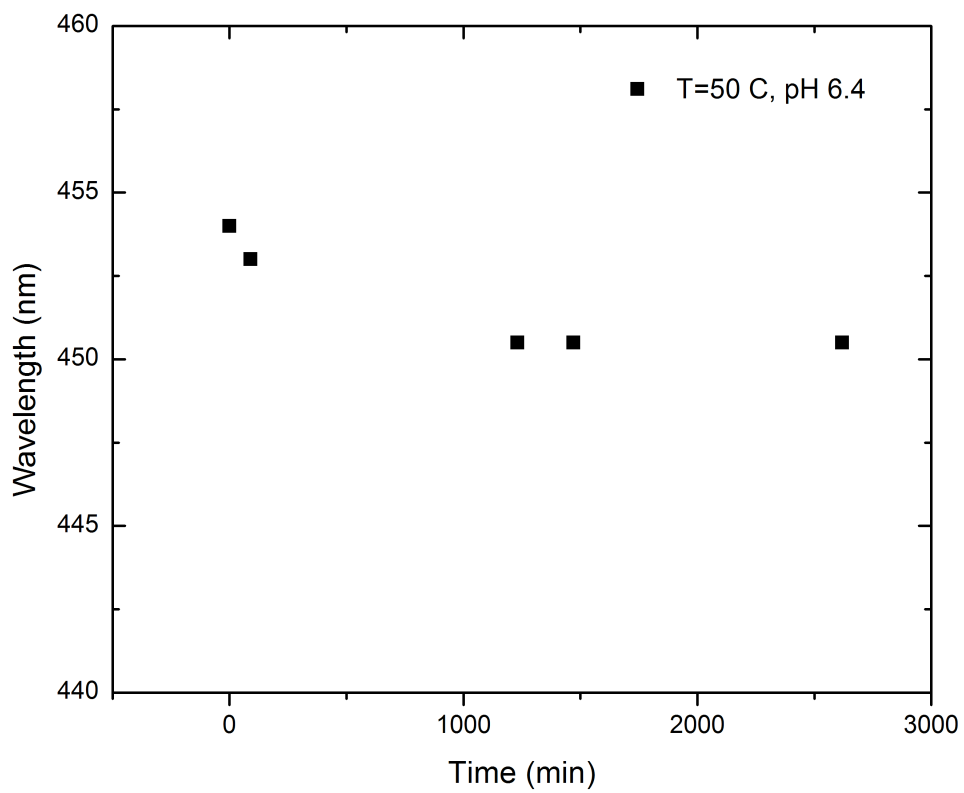


Figure 2.12 Effect of temperature on PANI and 0.25 mM H₂O₂ solution, without addition of HRP.

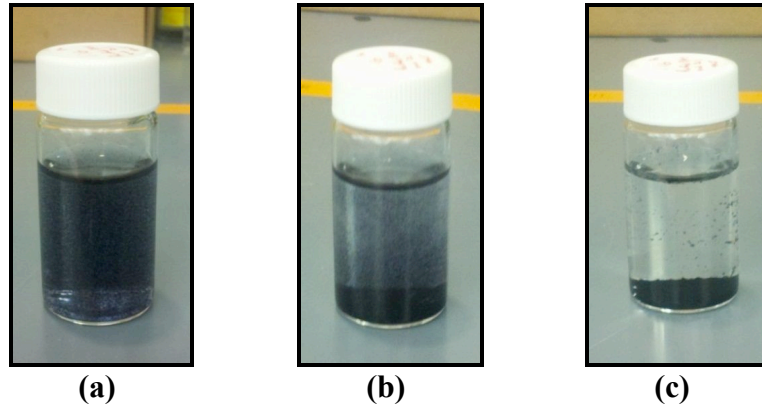


Figure 2.13 Images of PANI settling over time: (a) time=0; (b) time \approx 3 hours; (c) time \approx 18 hours (overnight).

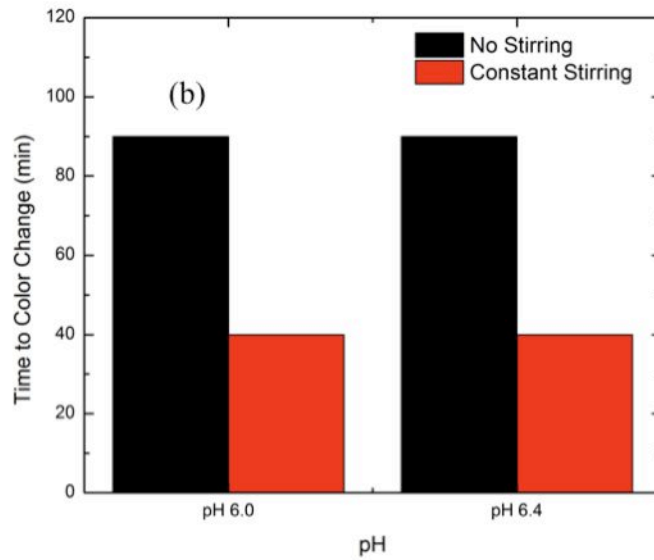
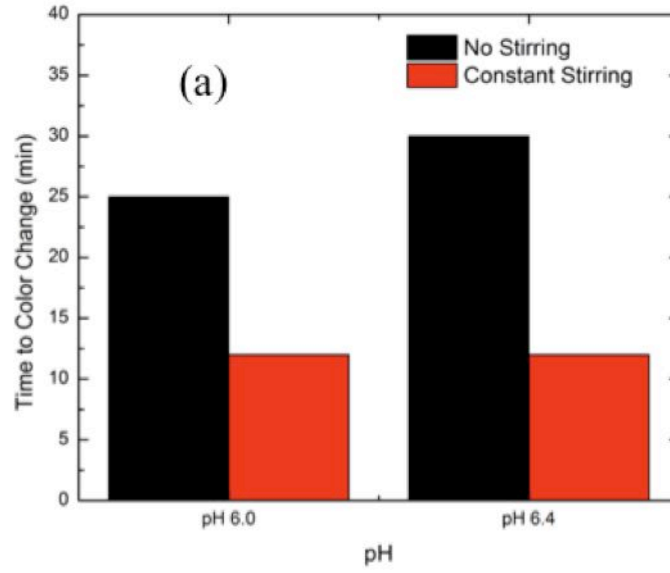


Figure 2.14 Effect of constant agitation on the time required for color change of PANI. While under constant agitation, the PANI solutions changed color twice as fast.

REFERENCES

- (1) Statistics from *Center for Disease Control (CDC) Estimates of Foodborne Illness in the United States: CDC 2011 Estimates*, February 2011, <http://www.cdc.gov/foodborneburden/>.
- (2) Rodriguez-Lazaro, D.; D'Agostino, M.; Herrewegh, A.; Pla, M.; Cook, N.; Ikononopoulos, J. Real-time PCR-based methods for detection of *Mycobacterium avium* Subsp paratuberculosis in water and milk. *Int. J. Food Microbiol.* **2005**, *101*, 93-104.
- (3) Jofre, A.; Martin, B.; Garriga, M.; Hugas, M.; Pla, M.; Rodriguez-Lazaro, D.; Aymerich, T. Simultaneous detection of *Listeria monocytogenes* and *Salmonella* by multiplex PCR in cooked ham. *Food Microbiol.* **2005**, *22*, 109-115.
- (4) Deisingh, A.; Thompson, M. Strategies for the detection of *Escherichia coli* O157 : H7 in foods. *J. Appl. Microbiol.* **2004**, *96*, 419-429.
- (5) Brooks, B.; Devenish, J.; Lutze-Wallace, C.; Milnes, D.; Robertson, R.; Berlie-Surujballi, G. Evaluation of a monoclonal antibody-based enzyme-linked immunosorbent assay for detection of *Campylobacter fetus* in bovine preputial washing and vaginal mucus samples. *Vet. Microbiol.* **2004**, *103*, 77-84.
- (6) Lazcka, O.; Del Campo, F. J.; Munoz, F. X. Pathogen detection: A perspective of traditional methods and biosensors. *Biosens. Bioelectron.* **2007**, *22*, 1205-1217.
- (7) Chattopadhyay, K.; Mazumdar, S. Structural and conformational stability of horseradish peroxidase: Effect of temperature and pH. *Biochemistry (N. Y.)* **2000**, *39*, 263-270.
- (8) Dolman, D.; Newell, G. A.; Thurlow, M. D.; Dunford, H. B. Kinetic Study of Reaction of Horseradish-Peroxidase with Hydrogen-Peroxide. *Can. J. Biochem.* **1975**, *53*, 495-501.
- (9) Matsunaga, I.; Shir, Y. Peroxide-utilizing biocatalysts: structural and functional diversity of heme-containing enzymes. *Curr. Opin. Chem. Biol.* **2004**, *8*, 127-132.
- (10) Veitch, N. Horseradish peroxidase: a modern view of a classic enzyme. *Phytochemistry* **2004**, *65*, 249-259.
- (11) Ryan, O.; Smyth, M. R.; Fagain, C. O. Horseradish peroxidase: The analyst's friend. *Essays in Biochemistry, Vol 28* **1994**, *28*, 129-146.
- (12) Krieg, R.; Halbhuber, K. Recent advances in catalytic peroxidase histochemistry. *Cell Mol. Biol.* **2003**, *49*, 547-563.

- (13) Piletsky, S.; Panasyuk, T.; Piletskaya, E.; Sergeeva, T.; El'skaya, A.; Pringsheim, E.; Wolfbeis, O. Polyaniline-coated microtiter plates for use in longwave optical bioassays RID D-2855-2009. *Fresenius Journal of Analytical Chemistry* **2000**, *366*, 807-810.
- (14) Stejskal, J.; Kratochvil, P.; Jenkins, A. D. The formation of polyaniline and the nature of its structures. *Polymer* **1996**, *37*, 367-369.
- (15) Batich, C.; Laitinen, H.; Zhou, H. Chromatic Changes in Polyaniline Films. *J. Electrochem. Soc.* **1990**, *137*, 883-885.
- (16) Souza, F. G., Jr.; Oliveira, G. E.; Anzai, T.; Richa, P.; Cosme, T.; Nele, M.; Rodrigues, C. H. M.; Soares, B. G.; Pinto, J. C. A Sensor for Acid Concentration Based on Cellulose Paper Sheets Modified with Polyaniline Nanoparticles. *Macromolecular Materials and Engineering* **2009**, *294*, 739-748.
- (17) Qasim, H.; Sadek, A. Z.; Arsat, R.; Wlodarski, W.; Belski, I.; Kaner, R. B.; Kalantar-zadeh, K. Optical and conductivity dependence on doping concentration of polyaniline nanofibers - art. no. 680012. *Device and Process Technologies for Microelectronics, Mems, Photonics and Nanotechnology Iv* **2008**, *6800*, 80012-80012.
- (18) Sengupta, P. P.; Adhikari, B. Influence of polymerization condition on the electrical conductivity and gas sensing properties of polyaniline. *Materials Science and Engineering A-Structural Materials Properties Microstructure and Processing* **2007**, *459*, 278-285.
- (19) Kim, B.; Koncar, V.; Devaux, E.; Dufour, C.; Viallier, P. Electrical and morphological properties of PP and PET conductive polymer fibers. *Synth. Met.* **2004**, *146*, 167-174.
- (20) Ji, S.; Li, Y.; Yang, M. Gas sensing properties of a composite composed of electrospun poly(methyl methacrylate) nanofibers and in situ polymerized polyaniline. *Sensors and Actuators B-Chemical* **2008**, *133*, 644-649.
- (21) Agbor, N.; Petty, M.; Monkman, A. Polyaniline Thin-Films for Gas-Sensing. *Sensors and Actuators B-Chemical* **1995**, *28*, 173-179.
- (22) Sengupta, P.; Barik, S.; Adhikari, B. Polyaniline as a gas-sensor material. *Mater. Manuf. Process.* **2006**, *21*, 263-270.
- (23) Collins, G. E.; Buckley, L. J. Conductive polymer-coated fabrics for chemical sensing. *Synth. Met.* **1996**, *78*, 93-101.
- (24) Krutovertsev, S.; Sorokin, S.; Zorin, A.; Letuchy, Y.; Antonova, O. Polymer Film-Based Sensors for Ammonia Detection. *Sensors and Actuators B-Chemical* **1992**, *7*, 492-494.

- (25) Agbor, N. E.; Cresswell, J. P.; Petty, M. C.; Monkman, A. P. An optical gas sensor based on polyaniline Langmuir-Blodgett films. *Sensors and Actuators B-Chemical* **1997**, *41*, 137-141.
- (26) Ji, S.; Li, Y.; Yang, M. Gas sensing properties of a composite composed of electrospun poly(methyl methacrylate) nanofibers and in situ polymerized polyaniline. *Sensors and Actuators B-Chemical* **2008**, *133*, 644-649.
- (27) Huang, J. X.; Kaner, R. B. A general chemical route to polyaniline nanofibers. *J. Am. Chem. Soc.* **2004**, *126*, 851-855.
- (28) Nicolas-Debarnot, D.; Poncin-Epaillard, F. Polyaniline as a new sensitive layer for gas sensors. *Anal. Chim. Acta* **2003**, *475*, 1-15.
- (29) *Enzyme handbook*, 7th ed.; D. Schomburg, M. S., Salzmann, M., Eds.; Springer-Verlag: Berlin ; New York, 1998 .
- (30) Moon, D.; Ezuka, M.; Maruyama, T.; Osakada, K.; Yamamoto, T. Kinetic-Study on Chemical Oxidation of Leucoemeraldine Base Polyaniline to Emeraldine Base. *Macromolecules* **1993**, *26*, 364-369.

CHAPTER 3: Solid Based Detection System

3.1 Introduction

This chapter focuses on the beginning stages towards the development a colorimetric chemical warfare agent detector utilizing polyaniline (PANI). We attempt to graft PANI to two substrates with considerably different glass transition temperatures T_g using a silane coupling agent. We use polydimethylsiloxane (PDMS) and polypropylene (PP) as our two substrates and 3-(phenylaminopropyl)trimethoxysilane (PAPTMOs) as our silane coupling agent. We are investigating two substrates with different T_g 's to determine the effect of T_g on the colorimetric response time. We expect the response time for the substrate with the lower T_g , PDMS, to be faster due to its inherent polymer backbone flexibility allowing the grafted colorimetric response to quickly rearrange for optimal contact with a probing media such as ammonia.

3.1.1 Polydimethylsiloxane and polypropylene

Polydimethylsiloxane is a silicone rubber with low density, high hydrophobicity, and low conductivity¹ comprising a T_g of 145-150 K.² It comprises an alternating Si-O-Si backbone with two methyl groups bound to the silicone (see Figure 3.1a). PDMS has broad application in microfluidic devices,³ insulation, anticorrosion, and antifouling coatings.⁴ Additionally, Hiamtup et al. dispersed PANI in a PDMS matrix, however the PANI was not bound to the PDMS.⁵ This was done to study electrorheological effects of PANI in PDMS for potential uses as vibration dampers or clutches. When an electric field was applied to the composite, the material stiffens and only a percentage of the flexibility was recovered when the electric field was removed.

Polypropylene (PP) (see Figure 3.1b) is a versatile thermoplastic that is processed in large quantities by major fabrication processes such as molding, extrusion, film, and fiber technology. Major applications of PP include pipe and automobile parts, filtration media, and nonwovens.⁶ PP comprises a carbon backbone with a methyl group bound to every other carbon in the backbone with a T_g of 373K.⁷

3.1.2 Previous work on grafting PANI

Due to the previously mentioned properties of PANI, many research groups have grafted PANI to various substrates. Anbarasan et al. reported a method to chemically graft aniline on poly(ethylene terephthalate) (PET) fiber and Nylon 6-6 fiber. Their method required that the fiber be soaked in hydrochloric acid prior to the addition of monomer and oxidant.^{8, 9} Lei et al. utilized γ -(2,3-epoxypropoxy)propyltrimethoxysilane (EPTMS) as a coupling agent on nano silica. The EPTMS modified silica was reacted with aniline and then PANI was grafted via *in situ* chemical oxidative polymerization.¹⁰ Ji et al. developed a multiple step process to graft PANI on poly(tetrafluoroethylene) (PTFE) films. The steps included silylating PTFE with (p-aminophenyl)trimethoxysilane (APTS) and oxidative graft polymerization of aniline.¹¹ Li et al. also developed a multiple step process that led to PANI grafted to Si(100) wafers. The steps involved in this process include 1) hydroxylating the wafers, 2) silylate the wafer with phenyltrichlorosilane, 3) react with triflic acid to remove the benzene layer, 4) substituting the triflic acid with aniline, and finally 5) graft polymerization of PANI.¹²

Another method for grafting PANI to substrates is through the use of PAPTMS as a coupling agent. PAPTMS is a desirable coupling agent because one end of the coupling

agent will readily bind to hydrophilic surfaces, whereas the other end has an aniline moiety as a location to initiate PANI polymerization. Figure 3.1c shows the structure of PAPTAMOS. Wheelwright et al. utilized PAPTAMOS to graft PANI to silica¹⁴ and Wu et al. grafted PANI to glass slides and silicon wafers using PAPTAMOS.¹⁵ Both routes were successful as measured by FTIR, ¹³C Nuclear Magnetic Resonance (NMR), and X-ray Photoelectron Spectroscopy (XPS).

We propose a method to graft PANI to PDMS and PP via PAPTAMOS. This method does not require etching of the substrate surface, nor does it require additional substitution steps as an aniline moiety is already present on the coupling agent. We modify the substrate surface, silylate the surface, and then polymerize PANI from the surface. Figure 3.2 shows a schematic of the procedure.

3.2 Materials and Methods

3.2.1 Materials

Polypropylene (Exxon 3155) was obtained from Exxon Corporation in pellet form. The pellets were melt-pressed to discs at a temperature of 185° C. Polydimethylsiloxane was synthesized using Dow Corning Sylgard-184 elastomer kit. The Sylgard-184 elastomer kit contained two components, Sylgard-184A (base polymer) and Sylgard-184B (crosslinker plus catalyst). A mixture of 10:1 Sylgard-184A:Sylgard-184B by mass was stirred in a petri dish. Gentle vacuum was applied to remove air bubbles from the mixture and then cured for 24 hours at 75°C.¹ Post-cure, PDMS was extracted with toluene to remove any unreacted monomer. All other chemicals were used as received from Sigma Aldrich. For the polymerization of PANI and subsequent washing steps, aniline hydrochloride, ammonium

persulfate (APS), hydrochloric acid (HCl), 1-methyl-2-pyrrolidinone (NMP), and acetone were employed. Methanol (99.5% anhydrous) and 3-(phenylaminopropyl)trimethoxysilane (PAPTMOs) were required for the silylating reaction. Ammonia hydroxide (28-30%) was used for vapor sensing.

3.2.2 Ultraviolet Ozone (UVO) Treatment

The surfaces of PP and PDMS were modified via ultraviolet/ ozone (UVO) treatment using UVO cleaner model number T10X10/OES from Ultraviolet Ozone Cleaning Systems (UVOCS). Substrates were treated for 45 minutes on each side.

3.2.3 Silylation

After UVO treatment of the substrates, a silylation reaction was done with the treated substrates and the silane coupling agent, PAPTMOs. The reaction was done in a solution consisting of 20.4 g of PAPTMOs in 100 mL of methanol. The reaction was conducted at 85°C for 24 hours under reflux to ensure no loss of methanol. After 24 hours, each substrate was sonicated in 50 mL of methanol for 30 minutes to remove any non-reacted PAPTMOs.

3.2.4 Polyaniline graft polymerization

Polyaniline was grafted to the silylated substrates via chemical oxidative polymerization at 0°C using a procedure similar to that done by Wu et al.¹⁵ In a 20 mL vial, 0.194 g of aniline hydrochloride was dissolved in 10 mL of 1.2 M HCL to make an aniline solution with a concentration of 0.15 M. In a separate 20 mL vial, 0.342 g of APS was dissolved in 10 mL of 1.2 M HCL to make an APS solution with a concentration of 0.15 M. Both vials were placed in ice in a cooler for 2 hours. One silylated substrate was added to the vial with the aniline solution. The APS solution was then added to the aniline solution dropwise in direct contact with the substrate. The reaction vial remained on ice during the

polymerization reaction for 2.5 hours. The substrate was then removed from the reaction vial and placed in 50 mL of DI water and sonicated for 30 minutes to remove excess PANI not chemically bonded to the substrate.

To further verify that PANI was chemically bonded to the surface as opposed to being adsorbed on the substrate surface, the PANI grafted substrates were converted from the emeraldine salt (ES) form to the emeraldine base (EB) form of PANI. This was done because the EB form of PANI dissolves in NMP.^{11, 14-16} The PANI was converted to the EB form by placing the PANI grafted substrate in 50 mL of MilliQ water for 24 hours. MilliQ water was used because it acts as a weak base. A strong base will convert the PANI to the EB form, however strong bases will cleave the Si-O bond.¹¹ After conversion to the EB form, the PANI grafted substrate was placed in 50 mL of NMP and sonicated for 30 minutes to remove adsorbed PANI. The PANI grafted substrate was then placed in 10 mL of 1.2 M HCl to convert the EB form back to the ES form of PANI.

After conversion to the ES form of PANI, the PANI grafted substrates were exposed to ammonia hydroxide vapor. Ammonia hydroxide was poured into a 50 mL jar. The uncapped jar was placed in a fume hood and the PANI grafted substrate was held above the jar to observe the effect of vapor on the PANI.

3.2.5 Contact angle measurements

Static contact angle measurements were conducted via the sessile drop method using a Dataphysics Contact Angle System OCA20. Substrates were placed on a glass slide and the glass slide was then placed on the sample stage. A 2.0 μL drop was made with the syringe and the sample stage was raised to the drop and then lowered immediately after the

substrate made contact with the water drop. The contact angle was recorded 15 seconds after drop deposition. Measurements were taken at three different locations on each side of the substrate.

3.2.6 Fourier Transform Infrared Spectroscopy in the Attenuated Reflection Mode

Fourier Transform Infrared Spectroscopy in the Attenuated Reflection (FTIR-ATR) mode was conducted using a Thermo Fisher Nexus 470 FTIR with a germanium OMNI ATR crystal. Spectra were recorded after 64 scans at 2 cm^{-1} resolution.

3.3 Results and Discussion

3.3.1 UVO treatment of PDMS and PP

In order to successfully bond a silane coupling agent to a surface, the surface must have hydrophilic groups, for example -OH groups or -COOH groups.¹⁴ A common method for doing this is UVO treatment of substrates.^{1, 17} After modifying the surface of PP and PDMS, there was no visual difference in the substrates to suggest the UVO treatment was successful. In order to determine the success of the UVO treatment, two methods were employed: contact angle and FTIR-ATR. Contact angles greater than 90° indicate a hydrophobic surface, whereas contact angles less than 90° indicate a hydrophilic surface.¹⁸ Contact angle measurements were conducted prior to and after UVO treatment of PP and PDMS. Table 3.1 shows the results of the contact angle measurements for both sides of PP and PDMS in duplicate. The naming convention for the samples was Substrate-Sample Number-Side (e.g., PP-1-A refers to the first PP sample, side A). Contact angle measurements prior to UVO treatment clearly show the hydrophobic nature (contact angles greater than 90°) of both PP and PDMS and the contact angles agree with literature values.^{1,16} After UVO treatment, there was a significant drop in the contact angle values for

PP and PDMS. The contact angle for PP decreased an average of 45° , and the contact angle for PDMS decreased an average of 85° indicating successful modification (see Figure 3.3). FTIR-ATR spectra of PP and PDMS taken prior to UVO treatment were contrasted with the spectra taken following the UVO treatment to identify the formed hydrophilic groups. Figure 3.4 shows the FTIR-ATR spectra of PP before and after UVO treatment. Peaks of interest on the post-UVO treatment spectra are the peak located at 1708 cm^{-1} (C=O and COOH frequencies) and the broad peak located from 3115 cm^{-1} to 3600 cm^{-1} (hydroxyl groups (-OH)); these functionalities are the signature fingerprint of UVO treatment to polymers.¹⁹ The remaining peaks on the spectra are characteristic peaks of PP. Figure 3.5 shows the FTIR-ATR spectra of PDMS before and after UVO treatment. Like with the PP spectra, peaks of interest on the post-UVO treatment spectra were the peak located at 1712 cm^{-1} , associated with the hydrophilic moieties C=O and COOH, and the broad peak associated with hydroxyl groups located from 3100 cm^{-1} to 3604 cm^{-1} .¹⁹ These peaks indicated the UVO treatment was successful on the PDMS surface as previously demonstrated by others.⁴

3.3.2 Silylation of PP and PDMS

The UVO modified PP and PDMS were silylated with the silane coupling agent, PAPTMO. The methoxyl moieties of PAPTMO reacted with the hydrophilic groups on the UVO modified substrates, forming a bond between the substrate surface and the coupling agent, as proposed by Wheelwright et al.¹⁴

Static contact angle and FTIR-ATR measurements were conducted to verify the successful silylation of PP and PDMS. Using static contact angle, we expected the contact angles of the substrates to increase due to the presence of the benzene ring on the end of the

coupling agent that was not bound to the substrate.²⁰ Table 3.1 shows the static contact angle measurements of PP and PDMS before and after the silylation reaction. The contact angle measurements recorded before the silylation reaction were the same contact angles recorded after the UVO treatment. The contact angles for PP increased an average of 35°, however the magnitude of the increase in contact angle was not consistent on both sides of the PP. Both sides of both PP samples showed an increase in contact angle, indicating the silylation reaction was successful. The contact angle for PDMS increased an average of 72°, indicating the silylation reaction was successful. One side on one of the PDMS samples did not have a final contact angle as high as the other PDMS samples indicating less PAPTMOs was bound to the surface. Although the contact angle on this sample was not as high, there still was a significant increase in contact angle, indicating PAPTMOs was still bound to that side.

The resulting contact angle measurements after silylation for PP and PDMS samples were greater than 90°, indicating the surfaces were hydrophobic, which suggested the benzene ring on the coupling agent was exposed to the surface and would be available for PANI graft polymerization.²⁰ Figure 3.3 shows images of water droplets on the surface of the silylated surface indicating the more hydrophobic nature of the substrates following silylation.

Figures 3.6 and 3.7 show the FTIR-ATR spectra of PP and PDMS, respectively, following the silylation reaction. Peaks of interest were the peaks located at 1506 cm⁻¹, 1598 cm⁻¹, and 3400 cm⁻¹ on the spectra for PP and peaks located at 1504 cm⁻¹, 1601 cm⁻¹, and 3409 cm⁻¹ on the PDMS spectra. The peaks located near 1500 cm⁻¹ and 1600 cm⁻¹ were associated with aromatic rings, attributed to the benzene ring located on the PAPTMOs and

the peak located near 3400 cm^{-1} was associated with amines, which is present because of the N-H bond between the propyl chain and the benzene ring on the coupling agent.¹⁹ The presence of these three peaks indicated the successful bonding of the silane coupling agent to the surface of the PP and PDMS.¹⁴

3.3.3 Polyaniline graft polymerization

The PANI graft polymerization was conducted at 0°C to increase the selectivity of the surface polymerization rate from the PAPTMO modified PP and PDMS as compared to bulk polymerization. Previous work conducted by other groups concluded that the aniline moiety at the end of the coupling agent most likely reacts with aniline molecules or oligomers in the solution to form longer chains.^{15, 21}

In the polymerization of PANI, APS was dispensed directly onto the surface of the substrate to facilitate preferential radical formation on the substrate surface. Otherwise, the rate of reaction for bulk polymerization of aniline could be faster than the surface rate of reaction. During the APS addition to the aniline solution, the liquid turned from clear to pink to blue to green over a time span of approximately three minutes (see Figure 3.8) In contrast, PANI polymerization reactions performed at room temperature turned green almost immediately upon the addition of the oxidant consistent with the assumed slower reaction time 0°C versus 25°C .²²

Upon polymerization completion, the PP samples were dark green in color and the PDMS samples were light green. After sonication in DI water, both substrates remained green, although some PANI particles were visually observed in water for the PP substrate. After soaking in MilliQ water overnight, both substrates were blue. The blue substrates indicated the PANI was converted to the EB form.^{11, 14} When the converted PDMS substrate

was placed in NMP, the PANI instantly began dissolving. After 30 minutes, the PDMS substrate was clear and the NMP solution was clear as well. The clear PDMS substrate indicated the PANI was only adsorbed to the PDMS surface versus covalently bound. The PP had different results. After 30 minutes sonication in NMP, both the solvent solution and substrate remained blue. The blue NMP solution indicated the EB form PANI was dissolved in the NMP and the blue PP sample indicated PANI was still on the PP sample. To ensure the PANI remaining on the PP was grafted and not adsorbed, the PP sample was sonicated for another 30 minutes with fresh NMP. This was done to verify the NMP solution was not saturated with EB PANI and could no longer dissolve PANI from the PP sample. After additional sonication, the NMP solution was clear and the PP was blue, indicating the remaining EB PANI was indeed grafted to the surface of the PP. When the PANI grafted PP sample was placed in 1.2 M HCl to convert the PANI to the ES form, it instantly turned green upon contact with the HCl solution. Figure 3.9 shows images of each substrate following the polymerization reaction, sonication in DI water, conversion to EB form, sonication in NMP, and conversion to ES form (PP only). In image (c) of Figure 3.12, the EB form of PANI was already coming off the PDMS substrate. The substrate was accidentally placed in NMP prior to taking a photograph of the substrate. The substrate was in the NMP for no more than 2-3 seconds before it was taken out to get a photograph of the blue EB PANI on the surface. From the image, it is clear the PANI was not grafted to the surface of the PDMS.

Figure 3.10 shows the FITR-ATR spectra of the PANI grafted PP. There were two notable differences in the spectra of the PP silylated with PAPTMO₃S (PP-PAPTMO₃S) versus

the subsequent spectra of the PP grafted with PANI (PP-PANI). Namely, the peaks located at 1506 cm^{-1} and 1598 cm^{-1} were no longer present. The second difference was the appearance of a small peak located at 1660 cm^{-1} . There are three relevant functional groups that are associated with a peak at 1660 cm^{-1} : aromatics, amines, and imines.¹⁹ The aromatic peak is due to the benzene ring in the aniline repeat unit. The amine peak is attributed to the N-H that was located throughout the backbone. The imine peak came from a nitrogen bound between two carbons, to one carbon with a single bond, and to the other carbon with a double bond.

Figure 3.11 shows the FTIR-ATR spectra of the PDMS that was used in the PANI graft polymerization reaction. The spectra show the PDMS before the polymerization reaction and after the sonication with NMP. There is no change to the peaks located at 1504 cm^{-1} and 1601 cm^{-1} , the key identifying peaks of the coupling agent. Since the original peaks associated with the coupling agent remained, no Si-O bonds were cleaved during the conversion to the EB form or during the washing in NMP. It is not clear at this point why the reaction on the PDMS substrate did not proceed as on PP. We speculate that the accessibility of the benzene ring was reduced on the flexible Si-O backbone due to a preference to orient away from the polar solvent. Follow-up contact angle experiments with the polymerization solution as the probing media will be conducted to elucidate our conflicting results between the two substrates.

3.3.4 Exposure to ammonia hydroxide vapor

The PP-PANI was exposed to ammonia vapor to change the oxidation state of the PANI. The functionalized substrate changed from green to blue/blue-violet immediately upon being held over the open-end of the jar with ammonia hydroxide. The rapid color change indicated the oxidation state of PANI changed making our functional substrate a potential a vapor detector. Figure 3.9 shows a picture of PP-PANI after exposure to NH_4OH vapor.

3.4 Conclusions and future work

A new method for grafting PANI from a PP substrate was developed using a silane coupling agent, PAPTMOs. The silylation reaction was conducted at 85°C in a solution of methanol and PAPTMOs. The PANI graft polymerization was conducted at 0°C via chemical oxidative polymerization by adding the oxidant dropwise directly onto the substrate. Sessile contact angle and FTIR-ATR confirmed successful completion of each process step. Although PDMS was successfully silylated with PAPTMOs, the subsequent polymerization of PANI occurred in the bulk solution as opposed to being ‘grafted from’ the PDMS-PAPTMOs substrate.

The ultimate goal of this research was to develop a chemical warfare agent detector utilizing PANI as the detector. The next step in achieving this goal is to adapt the reported process to fibers. Therefore, a method for modifying the surface of fibers with hydrophilic groups will be investigated. After the surfaces of fibers are successfully modified, the fibers will be silylated with PAPTMOs. Polyaniline will then be grafted from the silylated fibers.

Finally, the PANI grafted fibers will be exposed to various vapors to determine detection limits and response times.

Additionally, a goal of this research was to compare detection response times of substrates with different polymer backbone mobility. Unfortunately, PANI was not successfully grafted to PDMS. As well as going further with applying the grafting process to PP fibers, work will continue to understand the grafting polymerization mechanism for an activated PDMS substrate. Polymerization methods that minimize the bulk while focusing the polymerization at the PDMS surface will be explored. For example, the polymerization can be done in a solution volume that barely covers the substrate and the oxidant would be added directly to the substrate surface. Another potential method would be to add a drop of the oxidant solution directly to the surface of the substrate and then add a drop of the monomer solution to the same spot. Once PANI is successfully grafted to the surface of PDMS, experiments can be conducted to compare the response times of PANI grafted PP and PANI grafted PDMS upon exposure to vapors.

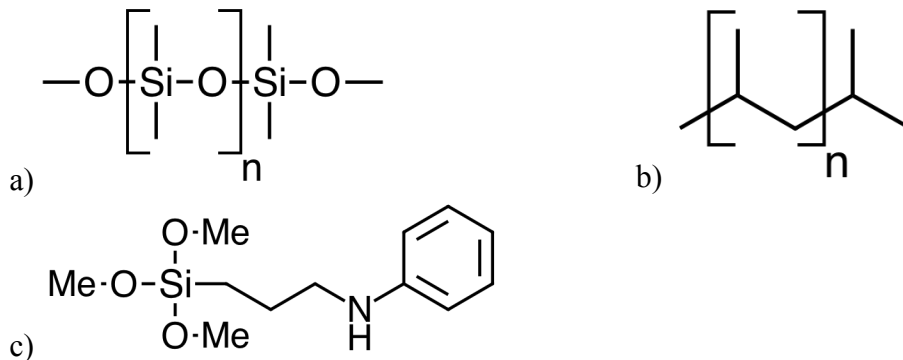


Figure 3.1 Chemical structures for the components of chemical sensors where a) polydimethylsiloxane (PDMS) and b) polypropylene (PP) are the substrates and c) 3-(phenylaminopropyl)trimethoxysilane (PAPTMO) is the silane coupling agent for subsequent surface grafting and polyaniline polymerization.

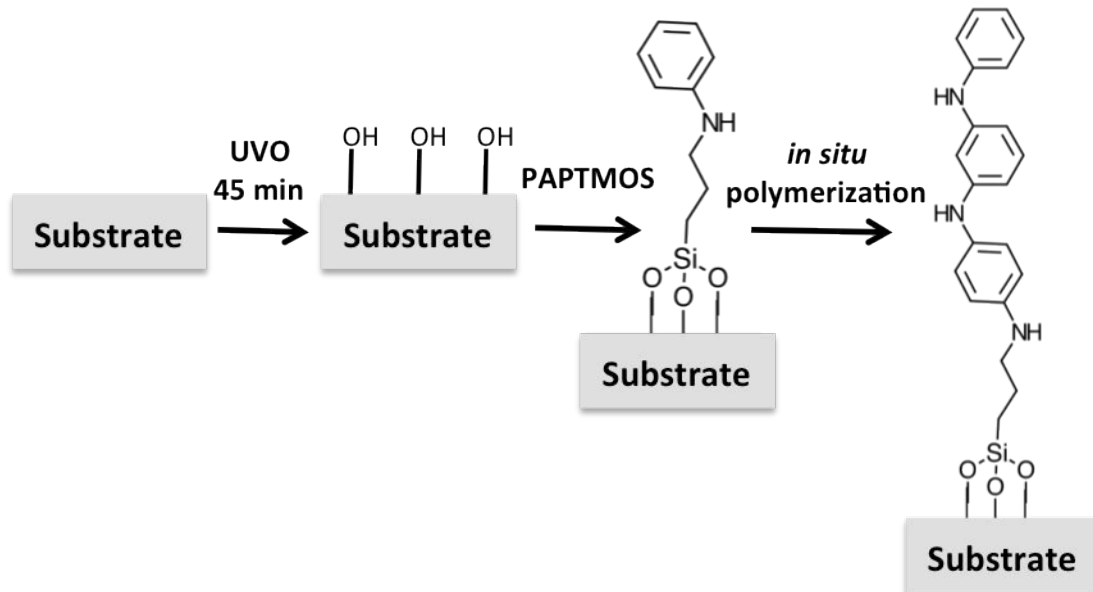


Figure 3.2 Graphical depiction of procedure to graft PANI to a substrate (PP or PDMS) using PAPTMOs. The substrate is treated with UVO for 45 minutes, generating hydrophilic groups (e.g. hydroxyls) on the surface. The modified substrate is silylated with PAPTMOs, and finally PANI is polymerized from the coupling agent.

Table 3.1 Average contact angles of PDMS and PP before UVO, after UVO, and after silylation with PAPTMOs, with standard deviation (SD).

Substrate	Before UVO	SD	After UVO	SD	After Silylation	SD
PDMS-1-A	113.3	3.2	26.8	8.7	106.0	3.3
PDMS-1-B	111.2	4.8	33.5	2.6	78.7	3.5
PDMS-2-A	109.9	3.0	24.0	3.9	102.1	2.2
PDMS-2-B	111.2	1.5	19.8	6.5	105.7	6.3
PP-1-A	95.1	10.3	52.7	6.3	97.1	6.7
PP-1-B	96.8	10.0	58.6	8.7	75.8	1.7
PP-2-A	106.0	0.8	52.1	3.9	103.1	3.2
PP-2-B	106.1	1.3	60.5	6.9	89.4	7.2

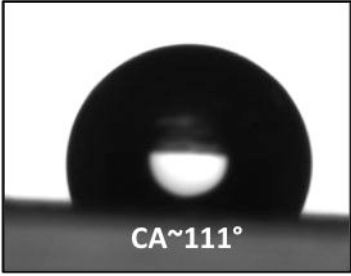
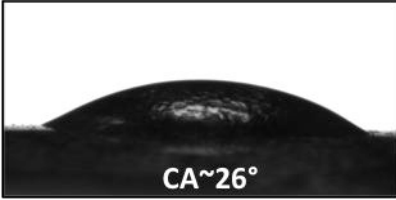
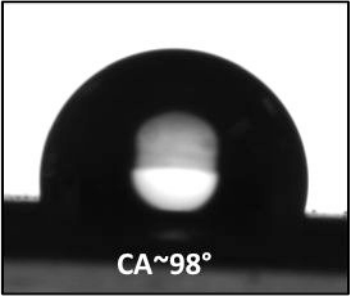
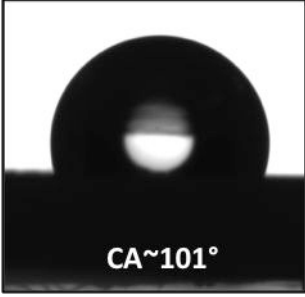
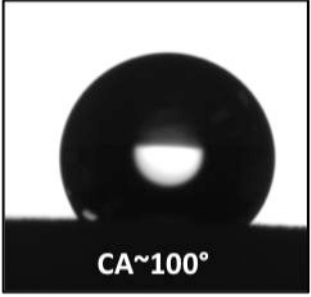
Substrate	Before UVO	After UVO	After Silylation
PDMS	 <p>a) CA~111°</p>	 <p>b) CA~26°</p>	 <p>c) CA~98°</p>
PP	 <p>d) CA~101°</p>	 <p>e) CA~56°</p>	 <p>f) CA~100°</p>

Figure 3.3 Images from the OCA20 obtained during measurement of static contact angle of PDMS (a-c) and PP (d-f) before UVO treatment, after UVO treatment, and after silylation. The actual contact angle is also shown.

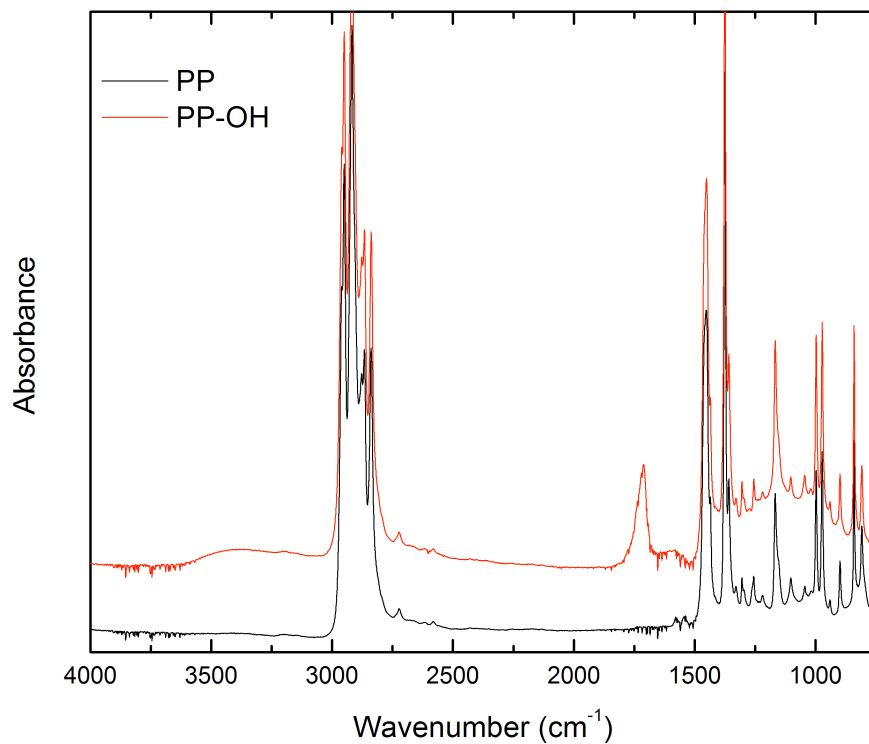


Figure 3.4 FTIR-ATR spectra of PP before and after UVO treatment. Peaks of note on the PP-OH spectrum are the peak located at 1708 cm^{-1} (C=O and -COOH) and the broad peak ranging from 3115 to 3600 cm^{-1} (-OH).

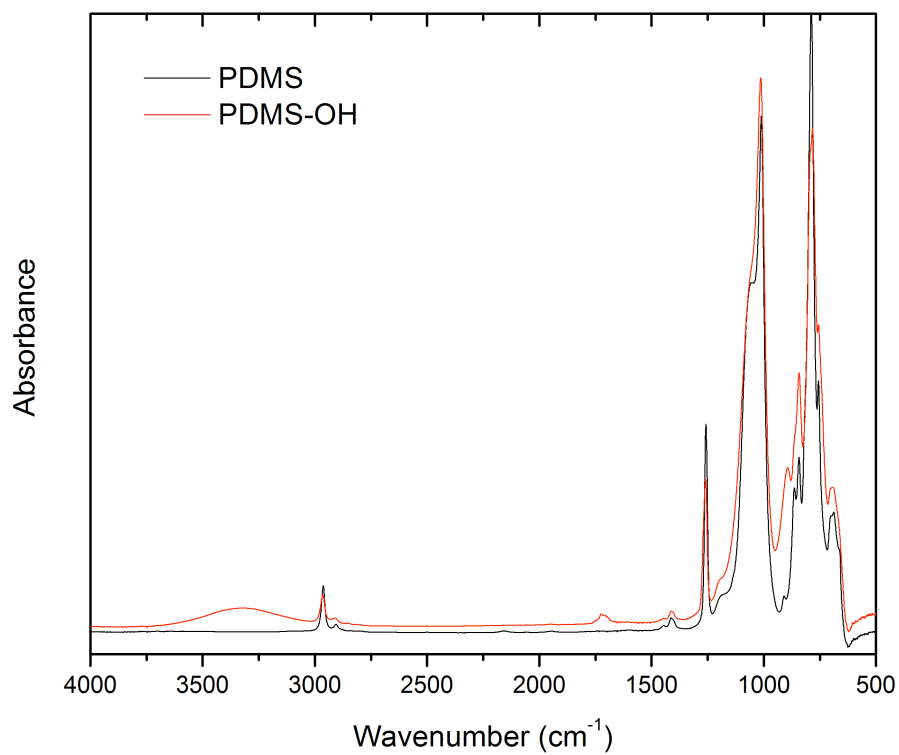


Figure 3.5 FTIR-ATR spectra of PDMS before and after UVO treatment. Peaks of interest on the PDMS-OH spectrum are the peak located at 1712 cm^{-1} (C=O and -COOH) and the broad peak located from $3100\text{ to }3600\text{ cm}^{-1}$ (-OH).

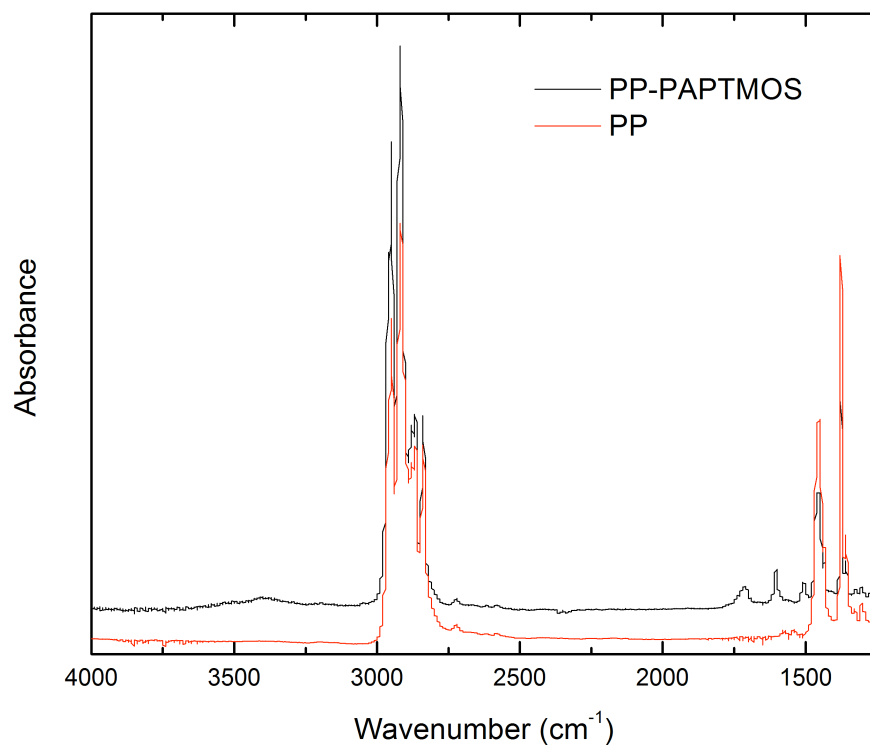


Figure 3.6 FTIR-ATR spectra of unmodified PP and PP after silylation. Peaks of interest on the PP-PAPTMOS spectrum are the peaks located at 1506 cm^{-1} and 1598 cm^{-1} (aromatic ring) and the broad peak centered on 3400 cm^{-1} (amine).

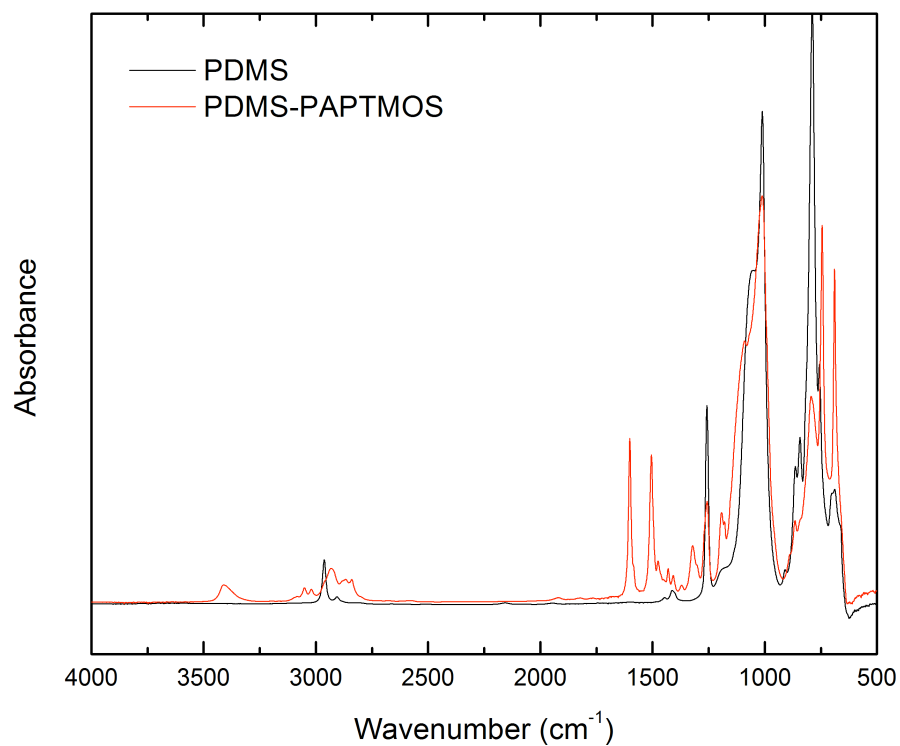


Figure 3.7 FTIR-ATR spectra of unmodified PDMS and PDMS after silylation. Peaks of interest on the PDMS-PAPT MOS spectrum are the peaks located at 1504 cm^{-1} and 1601 cm^{-1} (aromatic ring) and the peak at 3409 cm^{-1} (amine).

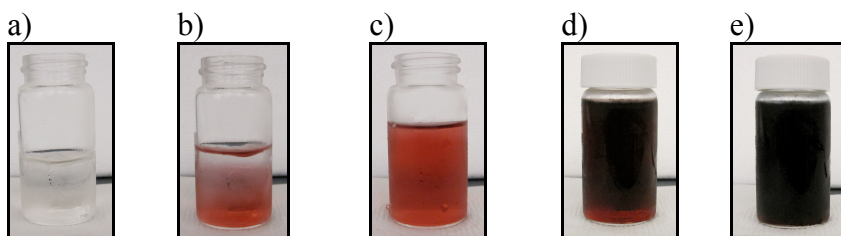


Figure 3.8 Images of the PANI polymerization reaction vial. Image (a) is the monomer solution with a substrate in it; (b) after addition of 1 mL oxidant solution; (c) after addition of more oxidant solution; (d) after addition of 10 mL oxidant solution; (e) approximately 3 minutes after beginning to add oxidant solution.

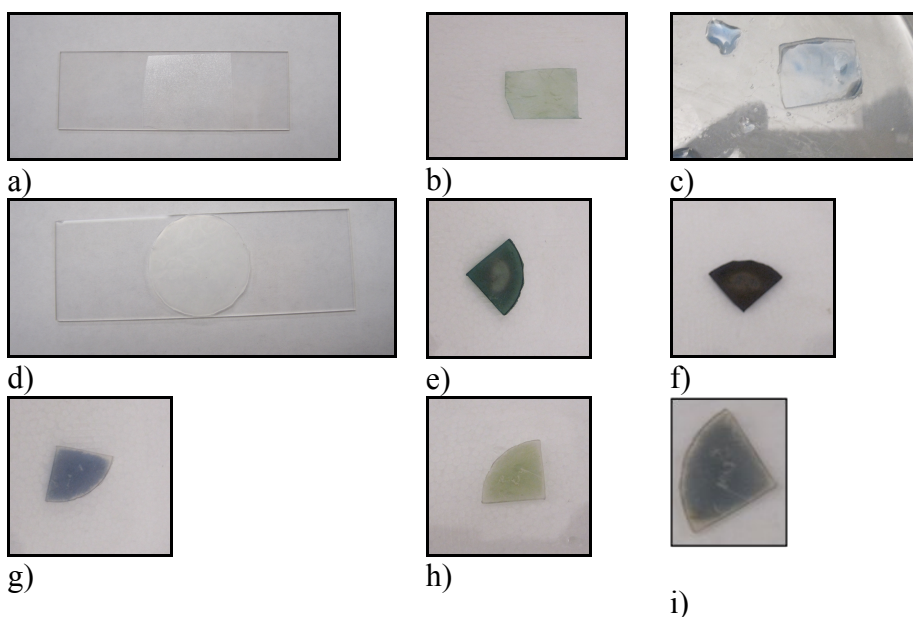


Figure 3.9 Images of PDMS (a-c) and PP (d-h) throughout the PANI grafting process. a) unmodified PDMS; b) PDMS after PANI polymerization; c) PDMS after conversion to EB form and after 2 seconds in NMP; d) unmodified PP; e) PP after PANI polymerization; f) PP after conversion to EB form; g) PP after sonication in NMP; h) PP after conversion to ES form; i) PP after exposure to NH_4OH vapor.

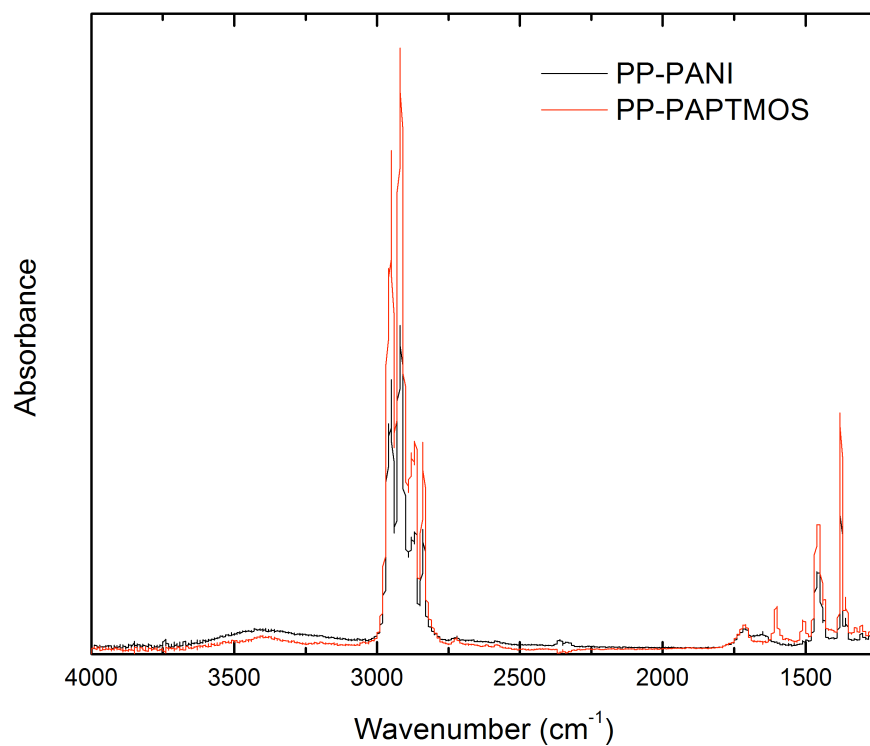


Figure 3.10 FTIR-ATR spectra of PP after silylation (PP-PAPTMOs) and after PANI polymerization (PP-PANI). The difference in the two spectra is the new peak at 1660 cm⁻¹ (aromatic, amines, and imines).

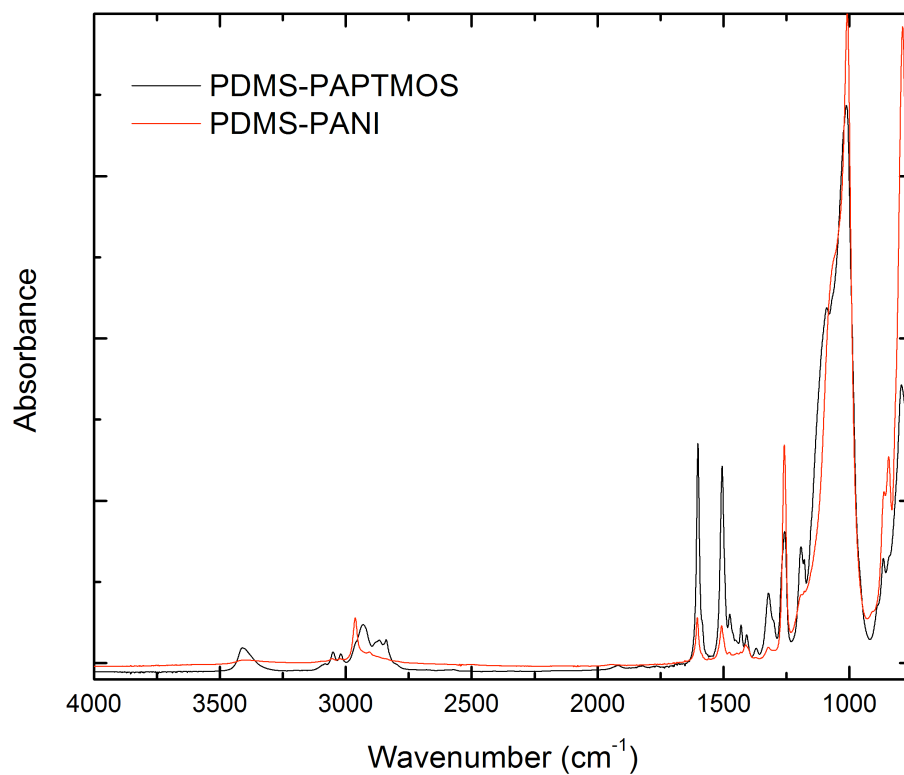


Figure 3.11 FTIR-ATR spectra of PDMS after silylation (PDMS-PAPTMOs) and after PANI polymerization (PDMS-PANI). There is no change to the peaks located at 1504 cm⁻¹ and 1601 cm⁻¹, indicating the coupling agent is still present on the PDMS surface.

REFERENCES

- (1) Efimenko, K.; Wallace, W. E.; Genzer, J. Surface modification of Sylgard-184 poly(dimethyl siloxane) networks by ultraviolet and ultraviolet/ozone treatment. *J. Colloid Interface Sci.* **2002**, *254*, 306-315.
- (2) Crowe-Willoughby, J. A.; Stevens, D. R.; Genzer, J.; Clarke, L. I. Investigating the Molecular Origins of Responsiveness in Functional Silicone Elastomer Networks. *Macromolecules* **2010**, *43*, 5043-5051.
- (3) Whitesides, G. M. The origins and the future of microfluidics. *Nature* **2006**, *442*, 368-373.
- (4) Efimenko, K.; Crowe, J. A.; Manias, E.; Schwark, D. W.; Fischer, D. A.; Genzer, J. Rapid formation of soft hydrophilic silicone elastomer surfaces. *Polymer* **2005**, *46*, 9329-9341.
- (5) Hiamtup, P.; Sirivat, A.; Jamieson, A. M. Electromechanical response of a soft and flexible actuator based on polyaniline particles embedded in a cross-linked poly(dimethyl siloxane) network. *Materials Science & Engineering C-Biomimetic and Supramolecular Systems* **2008**, *28*, 1044-1051.
- (6) McCrum, N. G. In *Principles of Polymer Engineering*; Buckley, C. P., Bucknall, C. B., Eds.; Oxford University Press: Oxford ; New York, 1997; .
- (7) Seymour, R. B. In *Polymer Chemistry : An Introduction*; Carraher, C. E., Seymour, R. B., Eds.; M. Dekker: New York, 1996; .
- (8) Anbarasan, R.; Muthumani, N.; Vasudevan, T.; Gopalan, A.; Wen, T. C. Chemical grafting of polyaniline onto nylon66 fiber in different media. *J Appl Polym Sci* **2001**, *79*, 1283-1296.
- (9) Anbarasan, R.; Vasudevan, T.; Kalaignan, G. P.; Gopalan, A. Chemical grafting of aniline and o-toluidine onto poly(ethylene terephthalate) fiber. *J Appl Polym Sci* **1999**, *73*, 121-128.
- (10) Lei, X.; Su, Z. Conducting polyaniline-coated nano silica by in situ chemical oxidative grafting polymerization. *Polym. Adv. Technol.* **2007**, *18*, 472-476.
- (11) Ji, L. Y.; Kang, E. T.; Neoh, K. G.; Tan, K. L. Oxidative graft polymerization of aniline on PTFE films modified by surface hydroxylation and silanization. *Langmuir* **2002**, *18*, 9035-9040.

- (12) Li, D.; Huang, J.; Kaner, R. B. Polyaniline Nanofibers: A Unique Polymer Nanostructure for Versatile Applications. *Acc. Chem. Res.* **2009**, *42*, 135-145.
- (13) Ruckenstein, E.; Li, Z. F. Surface modification and functionalization through the self-assembled monolayer and graft polymerization. *Adv. Colloid Interface Sci.* **2005**, *113*, 43-63.
- (14) Wheelwright, W. V. K.; Ray, S.; Eastal, A. J. A Novel Low Solvent Method for Grafting Polyaniline to Silylated Silica. *Polychar-18 World Forum on Advanced Materials* **2010**, *298*, 51-56.
- (15) Wu, C. G.; Yeh, Y. R.; Chen, J. Y.; Chiou, Y. H. Electroless surface polymerization of ordered conducting polyaniline films on aniline-primed substrates. *Polymer* **2001**, *42*, 2877-2885.
- (16) Zhong, W.; Deng, J.; Wang, Y.; Yang, W. Oxidative graft polymerization of aniline on the modified surface of polypropylene films. *J Appl Polym Sci* **2007**, *103*, 2442-2450.
- (17) Dasgupta, S. Surface Modification of Polyolefins for Hydrophilicity and Bondability - Ozonization and Grafting Hydrophilic Monomers on Ozonized Polyolefins. *J Appl Polym Sci* **1990**, *41*, 233-248.
- (18) Genzer, J.; Efimenko, K. Recent developments in superhydrophobic surfaces and their relevance to marine fouling: a review. *Biofouling* **2006**, *22*, 339-360.
- (19) Harris, D. C., In *Symmetry and Spectroscopy : An Introduction to Vibrational and Electronic Spectroscopy*; Bertolucci, M. D., Ed.; Dover Publications: New York, 1978.
- (20) Wu, C. G.; Chen, J. Y. Chemical deposition of ordered conducting polyaniline film via molecular self-assembly. *Chemistry of Materials* **1997**, *9*, 399-402.
- (21) Sawall, D. D.; Villahermosa, R. M.; Lipeles, R. A.; Hopkins, A. R. Interfacial polymerization of polyaniline nanofibers grafted to Au surfaces. *Chemistry of Materials* **2004**, *16*, 1606-1608.
- (22) Anbarasan, R.; Jayaseharan, J.; Sudha, M.; Gopalan, A. Peroxydisulfate initiated graft copolymerization of aniline onto poly(propylene) fiber - A kinetic approach. *J Appl Polym Sci* **2003**, *90*, 3827-3834.

CHAPTER 4: Conclusions and Future Work

4.1 Conclusions

In this work we discussed using the optical properties of polyaniline (PANI) as the basis for colorimetric sensing in two types of detector devices. The detector devices capitalized on the color changes associated with transitioning between the multiple oxidation states of PANI. We looked at utilizing a PANI dispersion for the detection of horseradish peroxidase (HRP) as a sensor for future use for pathogen detection. Additionally, we investigated using PANI in the solid form as a sensor by grafting PANI to polydimethylsiloxane (PDMS) and polypropylene (PP) using a silane coupling agent for future development as a colorimetric sensor that has potential to be utilized in chemical warfare agent detection.

4.1.1 Pathogen detection system

In Chapter 2, we discussed a proposed pathogen detection system, where PANI was dispersed in a dilute hydrogen peroxide (H_2O_2) solution. The detection system is based on HRP catalyzing the oxidation of organic compounds by hydrogen peroxide that is commonly used in bioassays.¹ Our detection system involved three main steps: 1) a substrate with an affinity for pathogens is exposed to a food sample by dipping or rubbing; if a pathogen is present in the food sample, the substrate will capture the pathogen; 2) the substrate is then exposed to a solution containing HRP conjugated to antibodies with an affinity for pathogens; if the substrate has a pathogen on it, the antibodies will bind to the pathogen and the substrate; 3) the substrate is then dipped into the PANI/hydrogen peroxide dispersion; if

HRP is present on the substrate, PANI will change color. Based on the proposed detection system, our objective was to assess the feasibility of using PANI as a detector for HRP.

In order to determine the feasibility of using PANI as an HRP detector, we created a dispersion of PANI and H_2O_2 . Above a certain concentration, hydrogen peroxide will oxidize PANI without the use of a catalyst like HRP. The goal for our sensor is to use the optical properties of PANI to indicate the presence of HRP. To do this, PANI cannot be completely oxidized by H_2O_2 prior to the addition of HRP. If PANI is completely oxidized by H_2O_2 , the addition of HRP will not cause further oxidation, or further color change. Therefore, we determined the concentration of H_2O_2 that would not fully oxidize PANI by itself and would maximize reaction kinetics upon addition of HRP. We first added PANI to solutions of varying H_2O_2 concentrations to determine concentration cut-off for PANI oxidation. Next, we added various concentrations of HRP to the PANI/ H_2O_2 dispersions to determine the optimum hydrogen peroxide concentrations for the fastest rate of oxidation and color change of the PANI. Finally, after determining the optimal H_2O_2 concentration, we investigated the effect of other reaction parameters, namely solution pH, temperature, and agitation.

We examined the effects of pH on the PANI dispersion across several fronts. We looked at how pH affects the PANI dispersion without H_2O_2 . We wanted to determine how increasing pH influenced the oxidation state of our PANI. Secondly, we added our optimal H_2O_2 concentration to the PANI dispersions in various pH buffers to determine if the pH affected the amount of oxidation from the H_2O_2 without the presence of HRP. Our last step

determined which pH buffers were the efficient at allowing HRP to catalyze the oxidation of PANI by hydrogen peroxide through the addition of HRP.

We expected the reaction rate to increase exponentially with an increase in temperature. We investigated the effect of temperature on the PANI/H₂O₂ dispersions by testing various temperatures without the presence of HRP to ensure increased temperature would not cause the hydrogen peroxide to further oxidize the PANI. Various concentrations of HRP were added at different temperatures to determine if increased temperature improved the reaction rate. We found that increasing temperature did increase the reaction rate of color change in the PANI dispersions.

Finally, we looked at the effect of constant agitation on the sensor. We found that over a period of several hours, PANI settled out of the dispersion. We conducted experiments at room temperature while maintaining the PANI dispersion at constant agitation. We found that maintaining the dispersion at constant agitation improved the time of color change by a factor of two.

4.1.2 Chemical warfare agent detection

In Chapter 3, we discussed grafting PANI to two substrates using a silane coupling agent with an aniline moiety. We aimed to compare the color changing response times after exposure to a vapor for substrates with two different glass transition temperatures. We hypothesized that the substrate with a lower T_g would have a faster response time due to ease of rearrangement and improved molecular movement. To meet this need, we investigated PP and PDMS. Our procedure consisted of four main steps: 1. Surface modification of the substrates with hydrophilic groups; 2. Silylation of modified substrates with the coupling

agent, 3-(phenylaminopropyl)trimethoxysilane (PAPTMOS); 3. Polymerization of PANI at site of coupling agent; and 4. Exposure of PANI grafted substrates to vapor.

Through the use of FTIR-ATR and static contact angle for verification, we were able to successfully modify the substrate surfaces with hydrophilic groups via UVO treatment and silylate the substrates with the silane coupling agent. We were able to successfully graft PANI on PP by conducting chemical oxidative polymerization of PANI at 0°C, however we were not successful in grafting PANI to PDMS. Finally, we exposed the PANI grafted PP to NH₄ vapor and observed the PANI change from green to violet within five seconds of exposure.

4.2 Future work

4.2.1 Pathogen detection system

Future work for the pathogen detection system remains focused on lowering the detection limit of HRP. We will investigate other conditions that may influence the oxidation of PANI. We will continue to look at the effect of constant agitation on the system. As reported, we have only observed constant agitation at room temperature. We will expand to observing higher temperatures at constant agitation. We will examine the effects of lowering the concentration of PANI with the hypothesis that at lower concentrations of HRP, PANI oxidation by H₂O₂ was still being catalyzed, however not all of the PANI present in the solution was being oxidized, so the color change was not visible. This may be negated through a lower PANI concentration. As we determine optimal individual reaction conditions, we will conduct experiments combining the factors to determine the overall optimum conditions for HRP, and thus pathogen, detection.

After determining optimal conditions for detecting free HRP, we will apply those conditions to the detection of conjugated HRP. After investigating various reaction conditions for conjugated HRP detection, we will examine HRP immobilized on a substrate similar to the one that will be used in the final pathogen detection system, as described in the proposed detection system.

4.2.2 Chemical warfare agent detection

In order for our findings from Chapter 3 to lead to a viable chemical warfare agent detector, several things need to be done. We need to further investigate a method for grafting PANI to PDMS to determine if T_g plays a role in sensor response time. Finding the optimal substrate for the sensor is a key parameter to the effectiveness of a detection system. The goal is to have a fiber based detector that can be integrated into a uniform; therefore we also will apply our methodology to fibers. To that end, we will research methods to modify the surfaces of fibers in preparation for the silylation reaction. Finally, a system to incorporate the PANI sensor needs to be developed, primarily to improve the selectivity of PANI. Exposure to an oxidizer or acid can cause PANI to change oxidation states, and color, providing a false positive. We envision this detection system consisting of multiple layers. Potentially, one layer would comprise a fiber mat immobilized with organophosphorus hydrolase (OPH). OPH is an enzyme that results in the hydrolysis of nerve agents that are organophosphorus compounds.^{2,3} The second layer would be a fiber mat grafted with PANI. After grafting PANI to the fibers, the PANI would be converted to the emeraldine base (EB) form (blue) or the violet pemigraniline base. PANI would need to be in the EB form because the hydrolysis reaction between OPH and nerve agents results in a drop in the pH to less than

pH 6. A drop in the pH would then cause the EB PANI fibers to transition to the emeraldine salt oxidation state, changing in color from blue or violet to green.

REFERENCES

- (1) Veitch, N. Horseradish peroxidase: a modern view of a classic enzyme. *Phytochemistry* **2004**, *65*, 249-259.
- (2) Russell, A.; Berberich, J.; Drevon, G.; Koepsel, R. Biomaterials for mediation of chemical and biological warfare agents. *Annu. Rev. Biomed. Eng.* **2003**, *5*, 1-27.
- (3) Gill, I.; Ballesteros, A. Degradation of organophosphorous nerve agents by enzyme-polymer nanocomposites: Efficient biocatalytic materials for personal protection and large-scale detoxification. *Biotechnol. Bioeng.* **2000**, *70*, 400-410.